New GRAAL data on nucleon photoabsorption in the nucleon resonance energy region

N.V.Rudnev, V.G.Nedorezov, A.A.Turinge for GRAAL Collaboration*
Institute for Nuclear Research RAS, Moscow, Russia
E-mail: rudnev@cpc.inr.ac.ru

GRAAL collaboration
GRenoble Accelerateur Anneau Laser

ESRF – European Synchrotron Radiation Facility , Grenoble

a Universit`a di Roma 2 ”Tor Vergata”, I-00133 Roma, Italy

b INFN Sezione di Roma 2 ”Tor Vergata”, I-00133 Roma, Italy

c Universit`a di Catania, I-95123 Catania, Italy

d INFN Laboratori Nazionali del Sud, I-95123 Catania, Italy

e IN2P3, Laboratoire de Physique Subatomique et de Cosmologie, 38026 Grenoble,France

f INFN Sezione di Genova, I-16146 Genova, Italy

g IN2P3, Institut de Physique Nucl´eaire d’Orsay, 91406 Orsay, France

h INFN Sezione di Torino, I-10125 Torino, Italy

i INFN Sezione di Roma I, I-00185 Roma, Italy

j INFN Sezione di Catania, I-95123 Catania, Italy

k Institute for Nuclear Research, 117312 Moscow, Russia

l INFN Laboratori Nazionali di Frascati, I-00044 Frascati, Italy

contents

1) Introduction

2) GRAAL facility – new quality of gamma beams and detectors

3) Experimental data on total photoabsorption in the nucleon resonance energy region for free and bound proton and neutron.

4) Interpretation of results in frame of the MAID – 2007.

5) New methods and perspectives.

Introduction

Amplitude for the photon Compton forward scattering on quasi-free nucleon :

$$f = \boldsymbol{\varepsilon}'^{*}\ \boldsymbol{\varepsilon}\ f_1(\omega) + i\ \omega\ \boldsymbol{\sigma}\ \boldsymbol{\varepsilon}'^{*} \times\ \boldsymbol{\varepsilon}\ f_2(\omega),$$

Where ε – invariant operator of the EM field,

σ – spin operator of the nucleon,

ω – photon energy.

At $\omega = 0$ (low energy theorem): $f_1(0) = -(\alpha\ /\ Z^2\ /\ M\ ),\ \ f_2(0) = (\alpha\ k^2\ /\ 2M^2\ ),$

Where *M – mass*, $\alpha = e^2\ /4\pi q hc = 1/137$, *eZ – electric charge*,

k - nucleon anomalous magnetic moment .

Free proton (Armstrong - 1972)

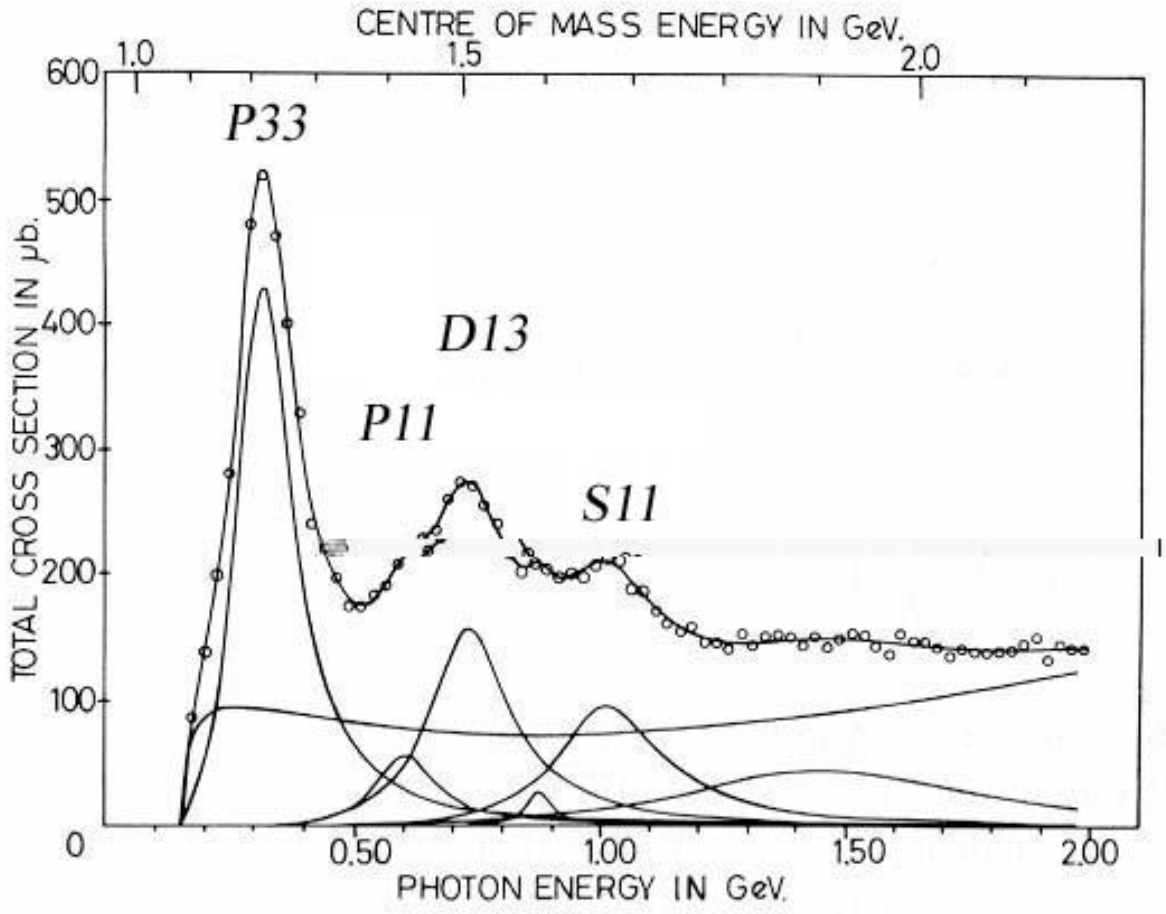

Fig. 7(b). Smooth fit to the measured data $\sigma_T{}^p$ in the resonance region.

Attempt to get the free neutron cross section (Armstrong-1972)

Subtraction of the proton contribution from the deuteron yield

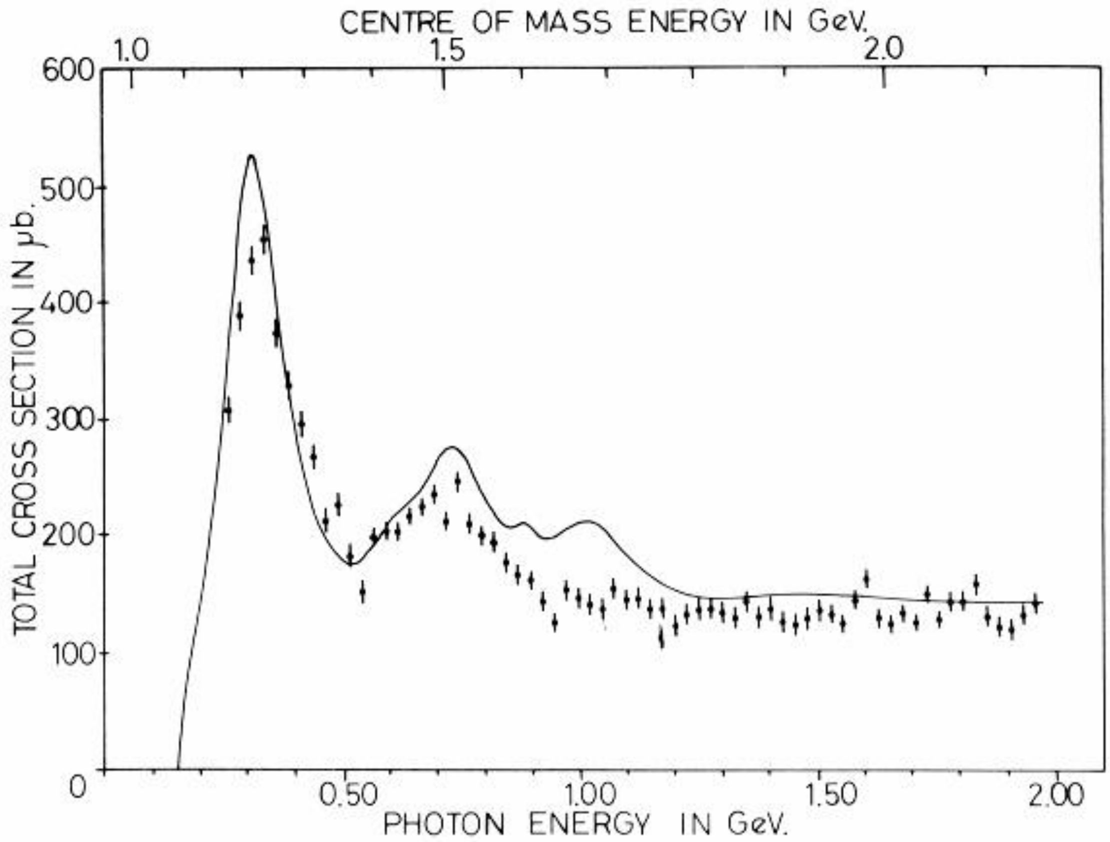

Fig. 8. This shows the values of $\sigma_T{}^n$ in the resonance region obtained by subtracting the measured $\sigma_T{}^p$ values from the deuterium values corrected for internal motion of the nucleons. The solid curve is the smooth fit to the measured $\sigma_T{}^p$ values.

Armstrong – Fermi correction

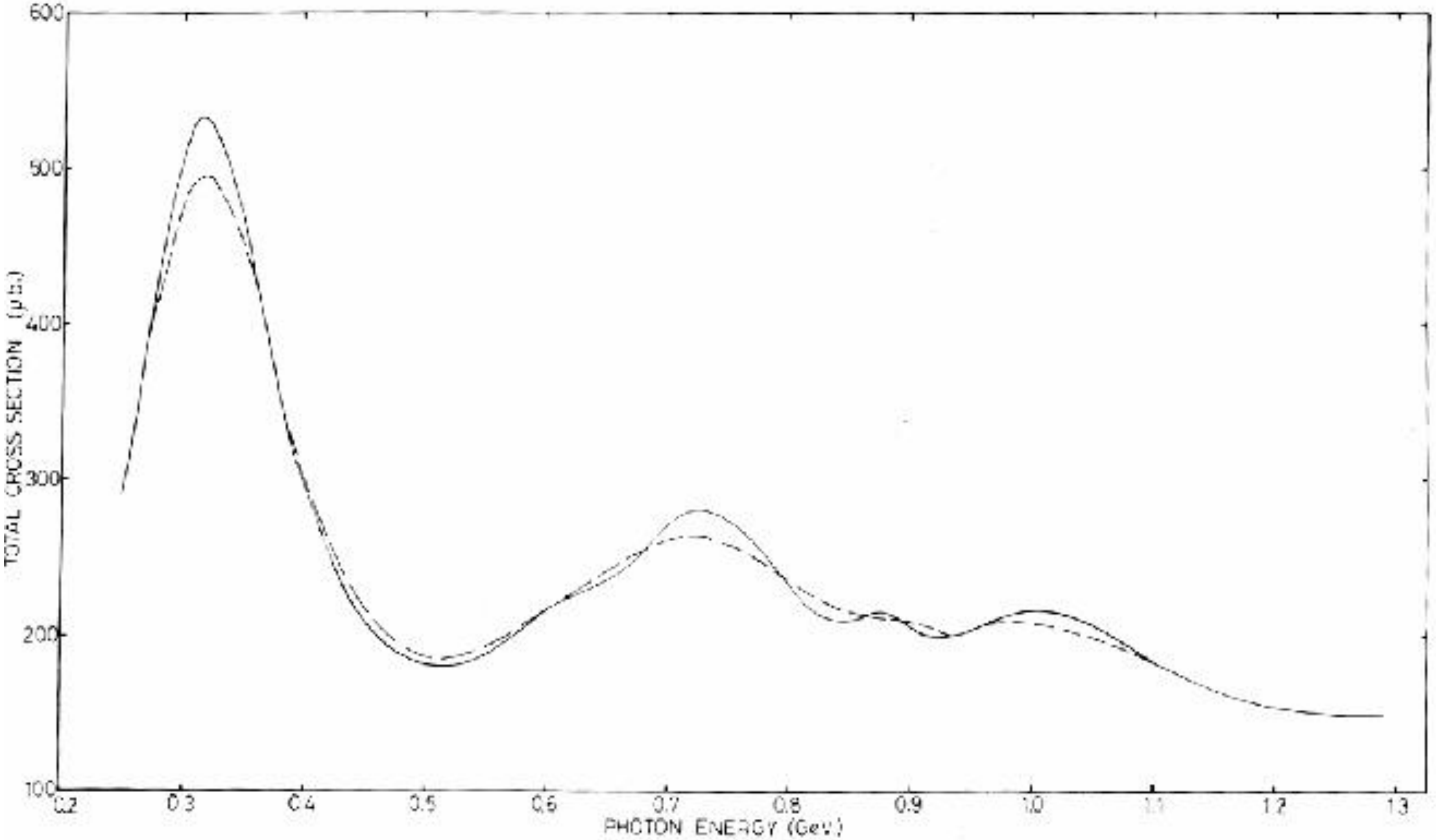

Fig. 6(b). The effects of internal nucleon motion are illustrated by smearing a smooth fit to the proton data (——) into a broadened curve (– – –).

458

T.A. Armstrong et al., Photon deuteron cross sections

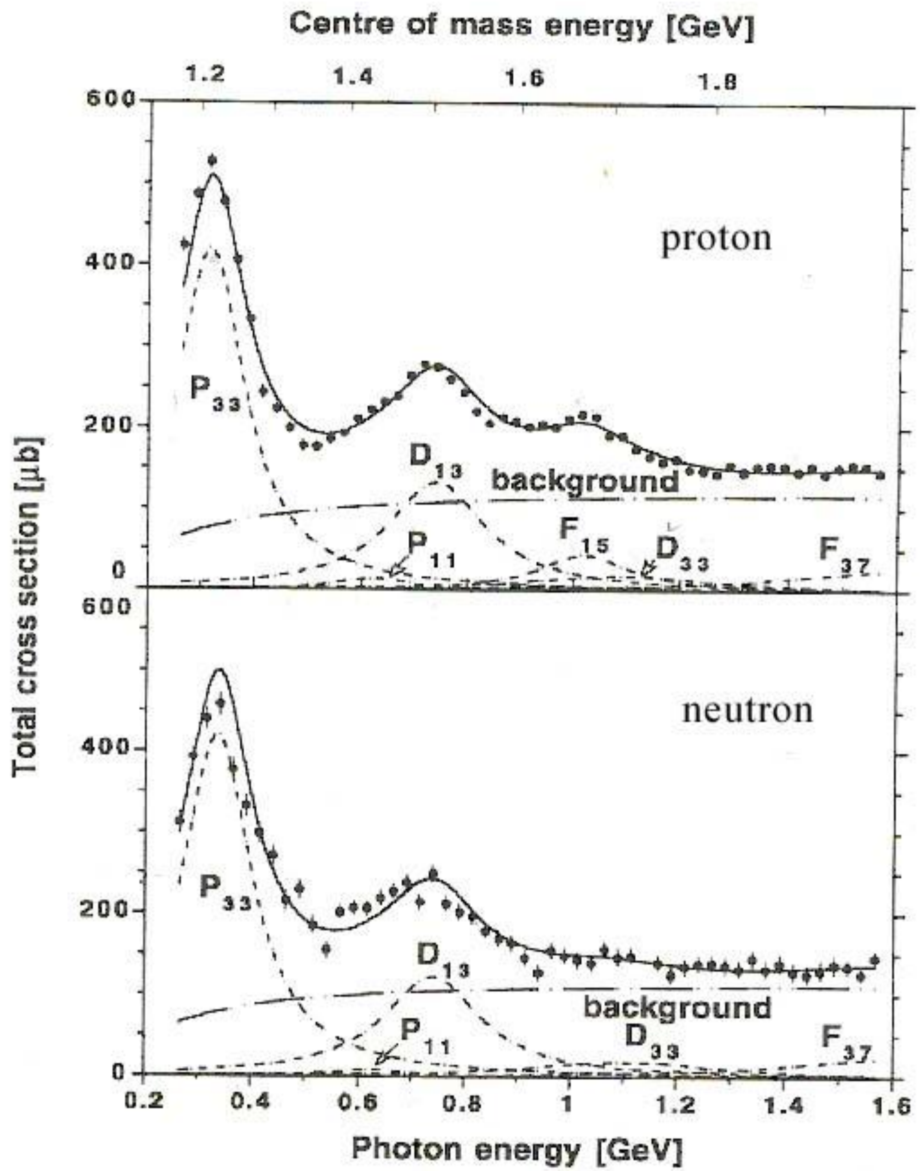

Centre of mass energy [GeV]
1.2
1.4
1.6
1.8
600
400
200
0
proton
P33
D13
background
P11
F15
D33
F37
600
400
200
0
neutron
P33
D13
background
P11
D33
F37
Total cross section [μb]
0.2
0.4
0.6
0.8
1
1.2
1.4
1.6
Photon energy [GeV]

Total photoabsorption on quasi-free nucleons (Mainz , Frascati - 1997) "Universal curve"

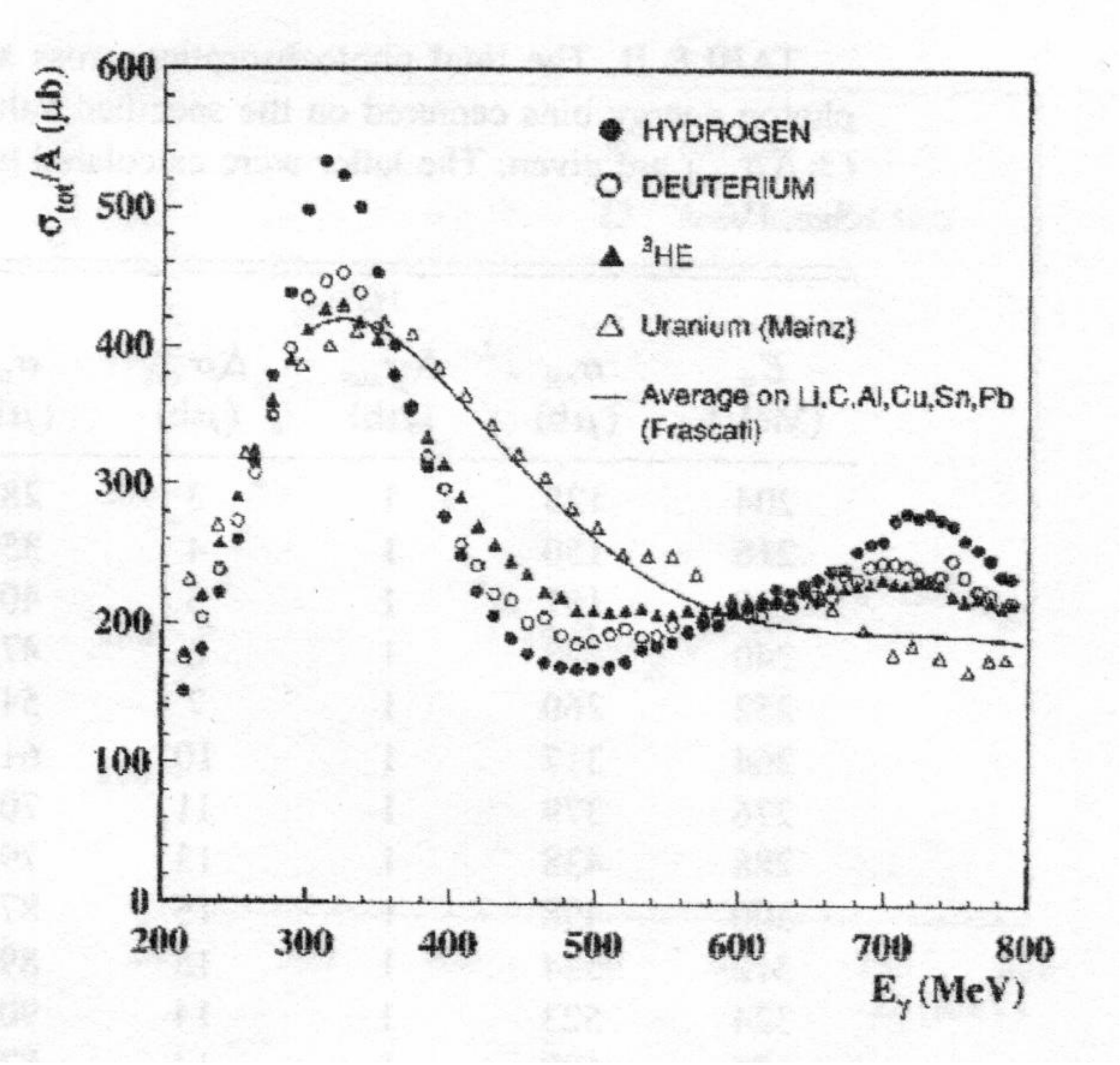

Actinide nuclei
(Novosibirsk VEPP-4 , CEBAF - 2000)

Free proton and neutron - dotted line

Actinide nuclei - solid line

Different nuclei with A = 7 – 238
(universal curve) – experimental points

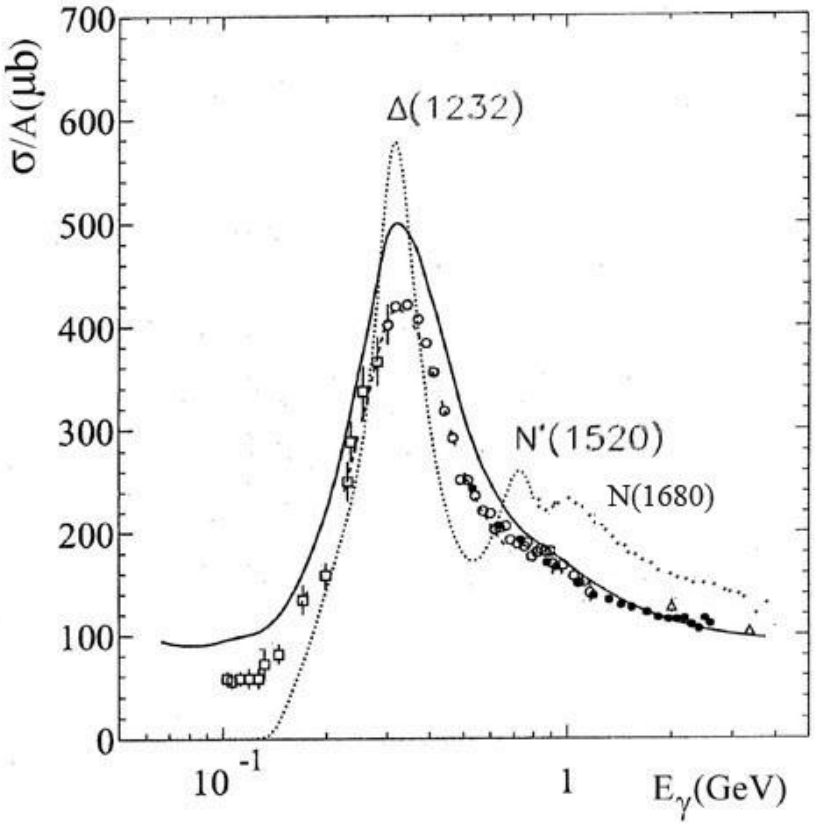

GRAAL

E_γ=600÷1500 MeV

ΔE_γ=16 MeV

P_γ≈100%

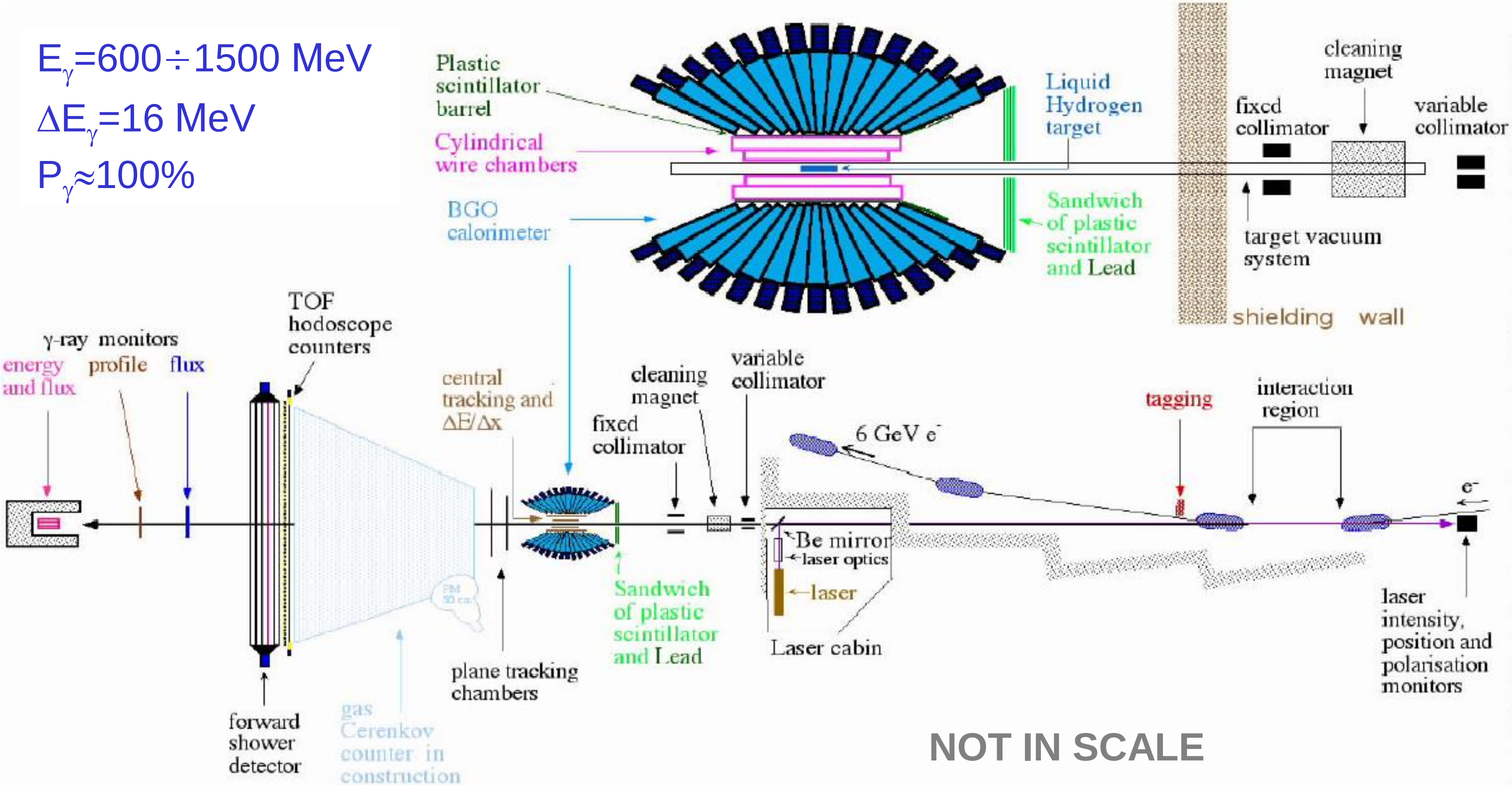

NOT IN SCALE

Backward Compton scattering

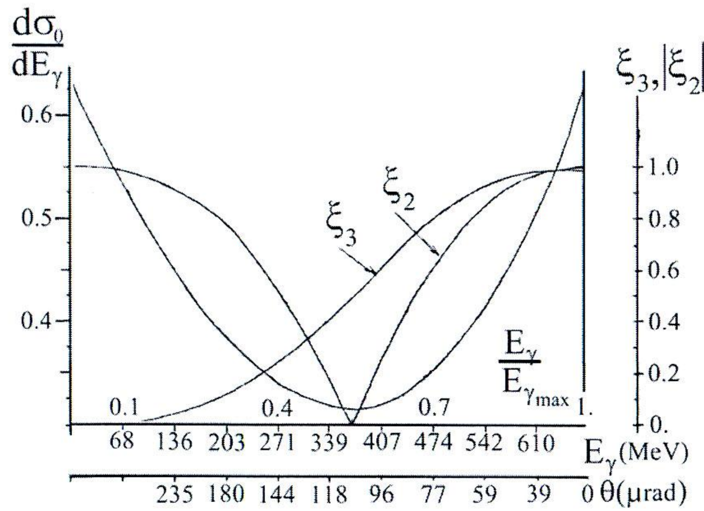

$$\frac{d\sigma}{dn} = 4\pi r_0^2 \left[\frac{K}{1+n} + \frac{1+n^2}{K} - \frac{4n^2}{(1+n^2)^2} \right]$$

Identification in BGO ball

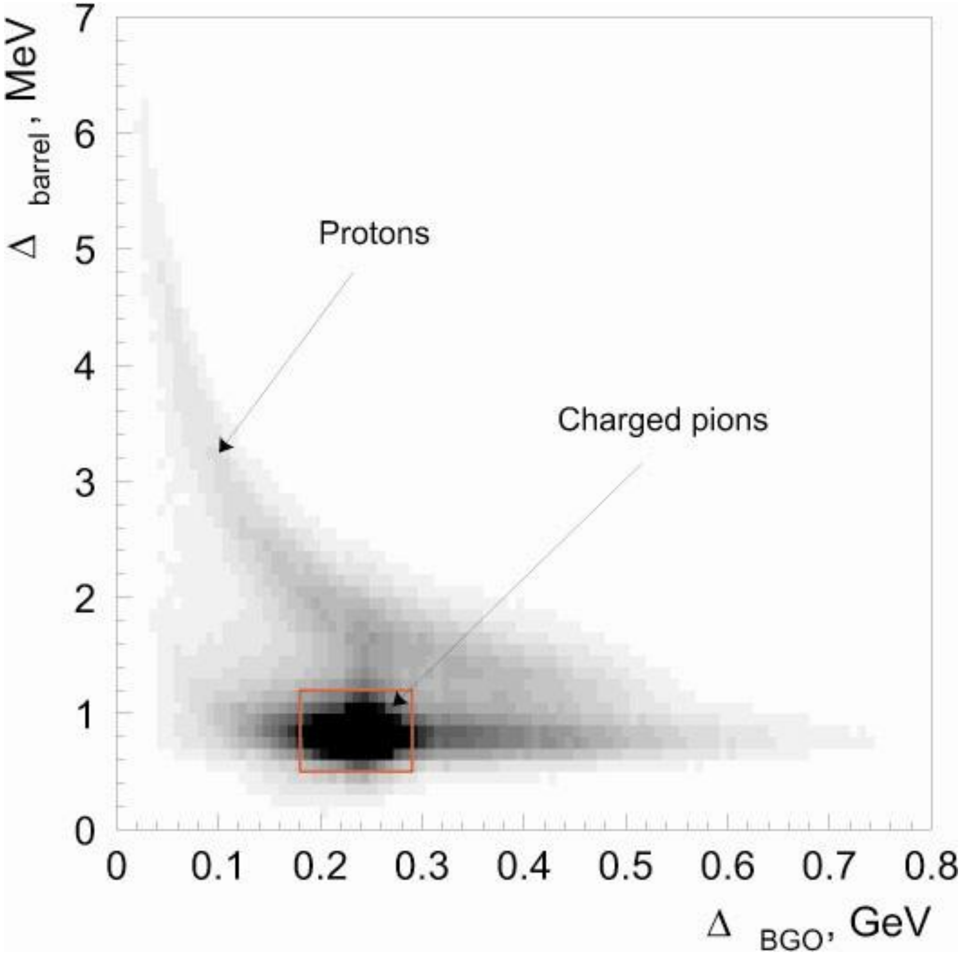

Identification in forward direction

ΔE – TOF

Identification and backgrounds

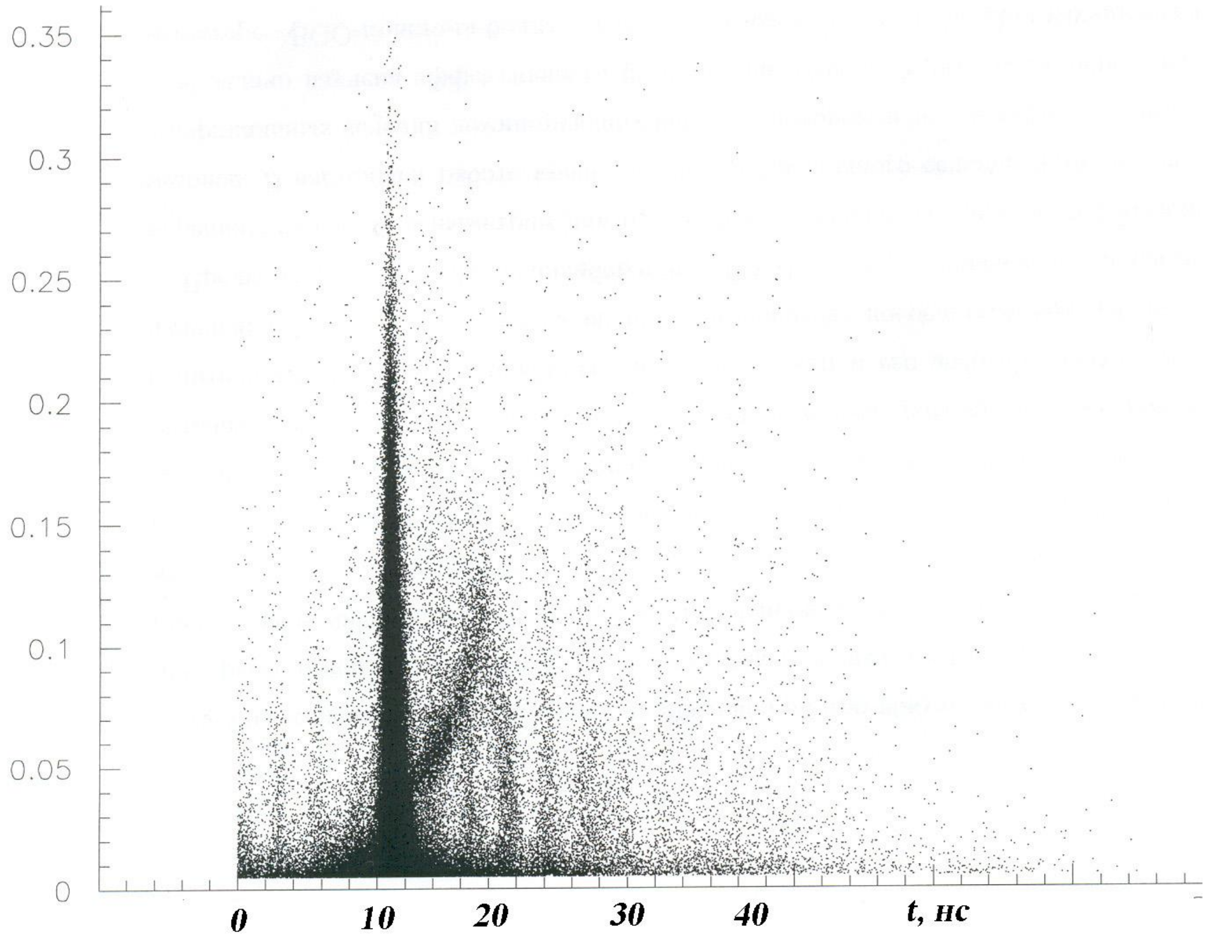

Time beam structure
Random coincidences

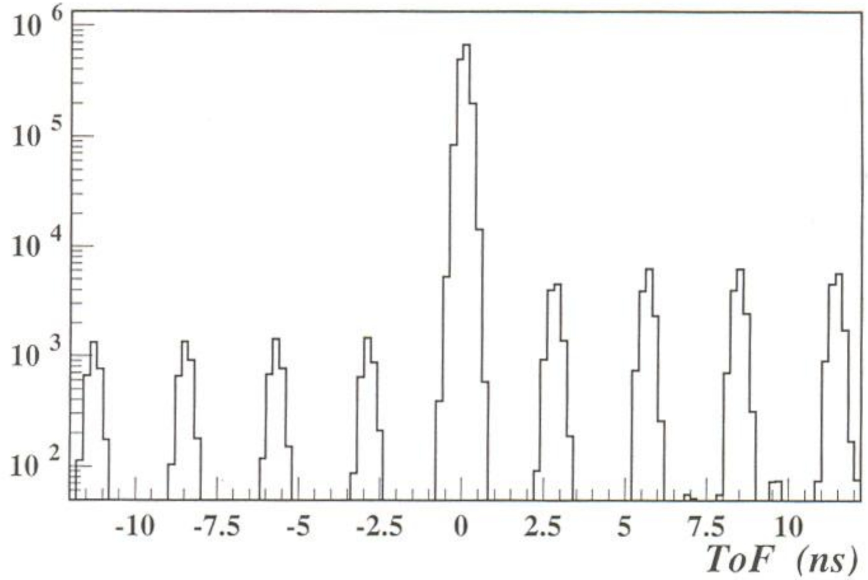

Spectre expérimental de temps de vol obtenu avec le moniteur fi

BACKGROUNDS

Angular θ-distribution for BGO events with MCLUS≤8 for the full (rhombs) and empty (squares) LH targets

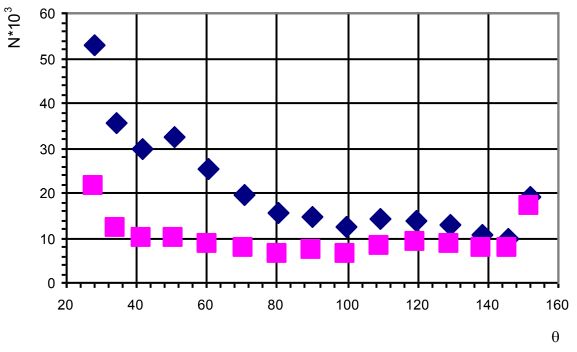

Experimental yield (rhombs) is the difference between full and empty targets yields.

Triangles correspond to the hadron yield evaluated by simulation.

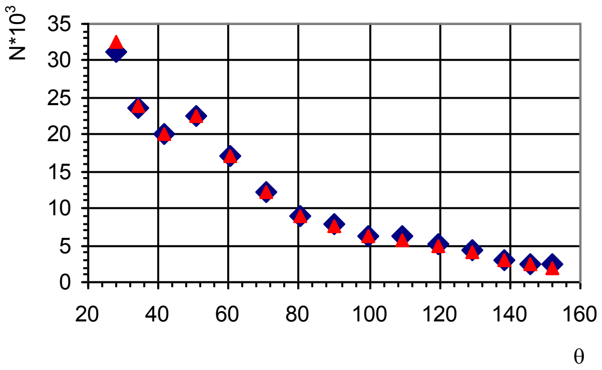

Subtraction Method

The total hadron yield

$$Y(E_\gamma) = N \cdot N_\gamma \cdot \sigma_{tot}(E_\gamma) \cdot \Omega(E_\gamma)$$

N is the number of nucleons target;
N_γ is the gamma flux,
σ is the total photoabsorption cross section;
Ω is the measurement efficiency (near 90%) evaluated by simulations.

Total yield - open points
Empty target yield - stars
Full points – difference

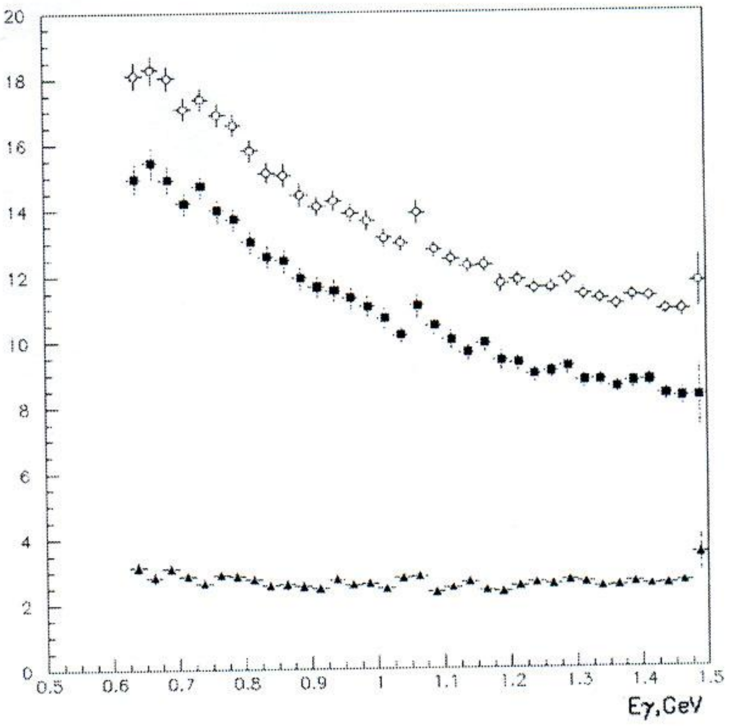

12-C target

Subtraction method

Simulation of experimental efficiency

Table 1

Simulated at 100 and 160 MeV thresholds as functions of E_γ.global BGO efficiencies

E_γ, GeV	0.55	0.65	0.75	0.85	1.05	1.15	1.25	1.35	1.45
$\Omega(E_\gamma \geq 100 MeV)$	0.86	0.88	0.90	0.89	0.88	0.90	0.90	0.90	0.90
$\Omega(E_\gamma) \geq 160 MeV)$	0.84	0.86	0.87	0.86	0.87	0.86	0.87	0.87	0.87

Summing method

Simulation of experimental efficiency

$$Y_{part}(E_\gamma) = N \cdot N_\gamma \cdot \sigma_{part}(E_\gamma) \cdot \Omega(E_\gamma)$$

N _ number of nucleons;

N_γ _gamma flux,

σ_{part} –partial cross section;

Ω - measurement efficiency evaluated by simulations.

In brackets the geometry efficiencies are shown

Table 2.
Simulated BGO efficiency for selected partial channels on the proton and neutron..
In parentheses the geometry efficiency is shown (see text).

.

E_γ, GeV	$\gamma p > \pi^+ n$	$\gamma p > \pi^0 p$	$\gamma p > \pi^+\pi^- p$	$\gamma p > \pi^0\pi^+ n$	$\gamma p > \pi^0\pi^0 p$	$\gamma p > \eta(2\gamma)p$
0.55	0.12(0.68)	0.44(0.72)	0.13(0.33)	0.031(0.29)	0.13(0.24)	
0.65	0.13(0.64)	0.42(0.71)	0.15(0.34)	0.037(0.29)	0.13(0.24)	
0.75	0.12(0.59)	0.35(0.64)	0.16(0.34)	0.038(0.29)	0.12(0.23)	0.008(0.00)
0.85	0.11(0.55)	0.25(0.56)	0.17(0.33)	0.034(0.28)	0.12(0.23)	0.052(0.10)
0.95	0.11(0.54)	0.19(0.52)	0.15(0.31)	0.031(0.26)	0.11(0.22)	0.069(0.14)
1.05	0.10(0.49)	0.13(0.50)	0.15(0.29)	0.027(0.25)	0.11(0.22)	0.066(0.14
1.15	0.09(0.44)	0.09(0.46)	0.16(0.28)	0.022(0.23)	0.10(0.21)	0.062(0.14)
1.25	0.08(0.41)	0.06(0.41)	0.17(0.26)	0.019(0.21)	0.10(0.21)	0.059(0.13)
1.35	0.07(0.40)	0.05(0.38)	0.17(0.24)	0.017(0.19)	0.10(0.20)	0.049(0.12)
1.45	0.06(0.38)	0.04(0.36)	0.17(0.22)	0.016(0.17)	0.10(0.18)	0.041(0.11)
	$\gamma n > \pi^- p$	$\gamma n > \pi^0 n$	$\gamma n > \pi^+\pi^- n$	$\gamma n > \pi^0\pi^- p$	$\gamma n > \pi^0\pi^0 n$	$\gamma n > \eta(2\gamma)n$
0.65	0.17(0.63)	0.13(0.70)	0.067(0.33)	0.094(0.30)	0.044(0.23)	
0.75	0.15(0.58)	0.12(0.64)	0.061(0.33)	0.091(0.29)	0.041(0.22)	0.005(0.00)
0.85	0.11(0.53)	0.093(0.54)	0.057(0.32)	0.086(0.27)	0.038(0.23)	0.033(0.10)
0.95	0.10(0.52)	0.076(0.51)	0.049(0.31)	0.077(0.25)	0.034(0.22)	0.051(0.15)
1.05	0.10(0.47)	0.071(0.49)	0.046(0.30)	0.068(0.23)	0.031(0.22)	0.047(0.15)
1.15	0.10(0.42)	0.067(0.46)	0.042(0.28)	0.058(0.23)	0.029(0.21)	0.045(0.14)
1.25	0.010(0.39)	0.061(0.41)	0.040(0.27)	0.050(0.22)	0.027(0.20)	0.041(0.13)
1.35	0.096(0.39)	0.047(0.39)	0.038(0.25)	0.047(0.21)	0.025(0.20)	0.038(0.12)
1.45	0.094(0.38)	0.043(0.38)	0.038(0.24)	0.045(0.21)	0.022(0.19)	0.034(0.11)

Simulation of efficirncy

Computer program chain -

LAGGEN (LAGrange GENerator) - event generator to evaluate angular distributions for reaction products basing on existing experimental data.

Geometrical efficiency – probability of particle to touch the detector.

LAGDIG (LAGrange DIGitation) – GEANT code for definite experimental conditions (thresholds, cluster size, cuts etc).

Instrumental efficiency - probability for the particle to be measured in accordance with the detector response function

PREAN (PRE-ANalysis).

Total efficiency - ratio of simulated events (obtained in accordance with the described above algorithm) to the total number of events simulated for selected reaction using the event generator.

Separation of the events for one charged pion photo-production on quasi-free nucleon
Red – experiment, green – simulation

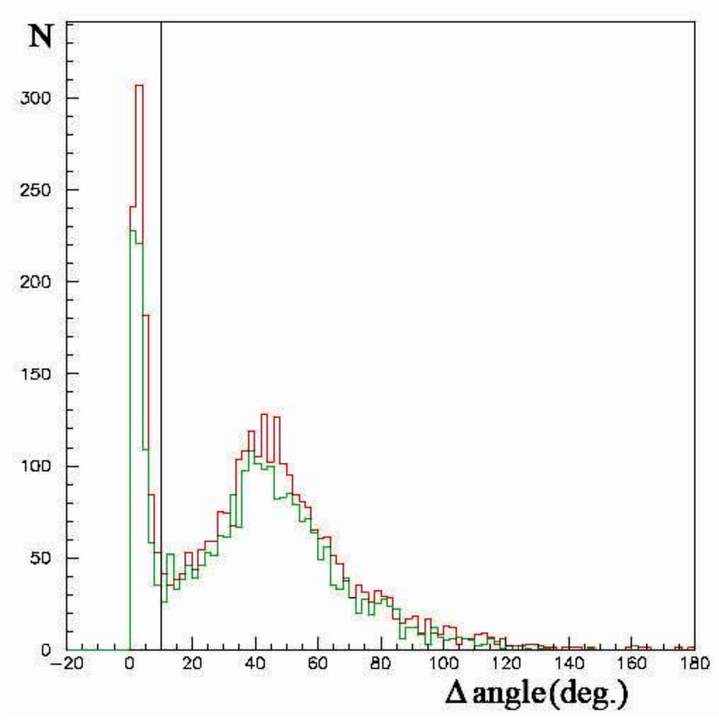

Angle between calculated and measured directions of the nucleon (reaction $\gamma n \Rightarrow p\pi^-$)

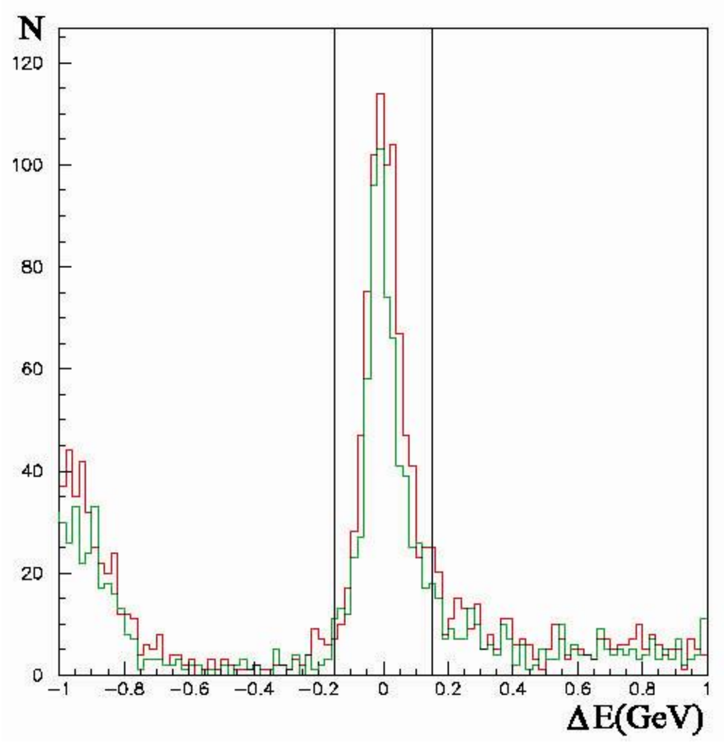

Difference between calculated and measured energies of the forward nucleon (reaction $\gamma n \Rightarrow p\pi^-$).

Here and later the black vertical lines specify the cuts for event selection

Separation of the events for one neutral pion photo-production on quasi-free nucleon
Red – experiment, green – simulation

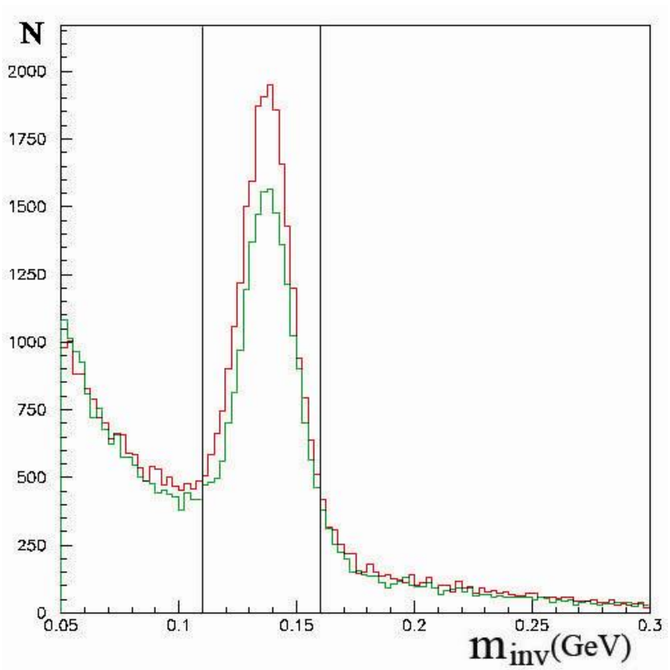

Invariant mass of two γ–quanta in BGO detector (reaction $\gamma p \Rightarrow p\pi^{0}$).

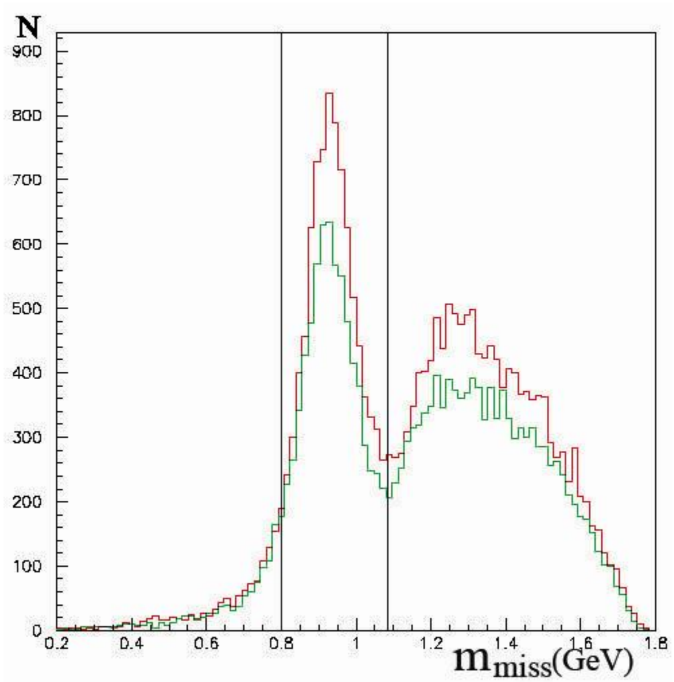

Missing mass of two g-quanta in BGO detector (reaction $\gamma p \Rightarrow p\pi^{0}$).

Separation of the events for η – meson photo-production on quasi-free nucleon
Red – experiment, green – simulation

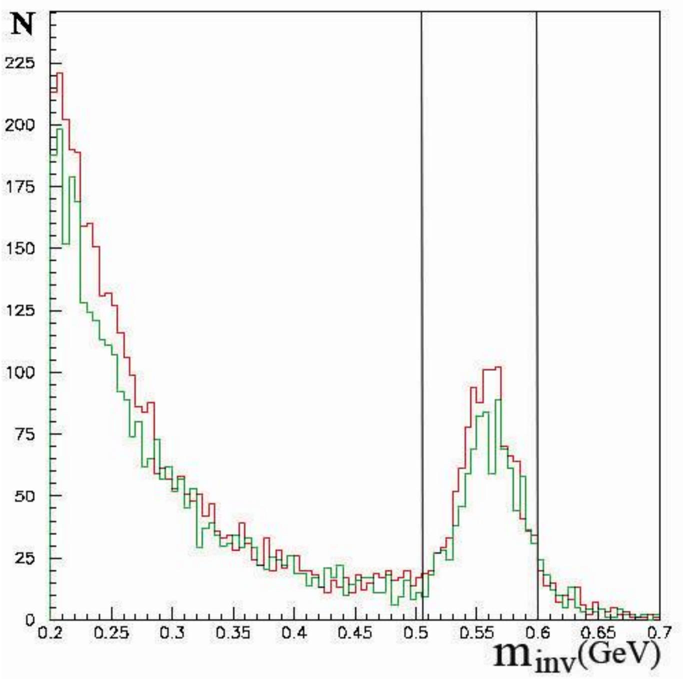

Invariant mass of two γ-quanta in BGO detector (reaction $\gamma p \Rightarrow p\eta$).

Separation of the events for double π^0 photo-production on quasi-free nucleon,
Red – experiment, green – simulation

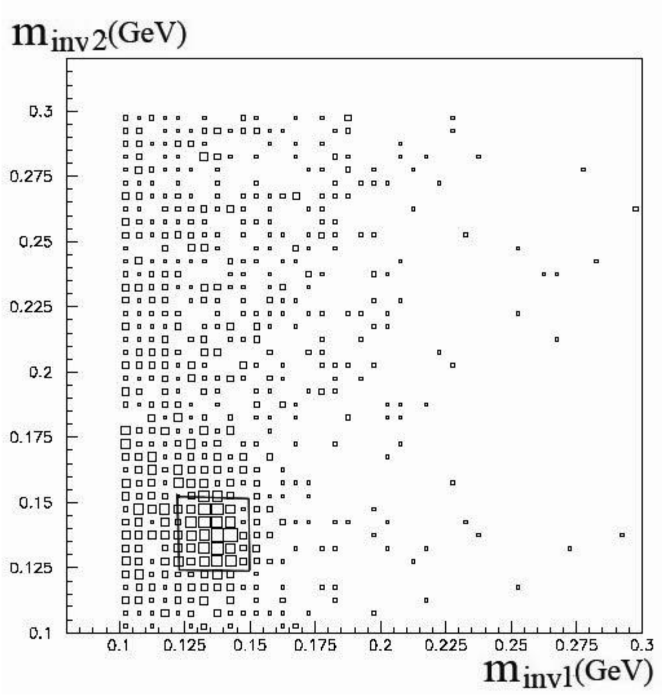

Invariant masses of two pairs of γ-quanta (reaction $\gamma p \Rightarrow p\pi^0\pi^0$). Rectangle marks area of the selected events.

Cross section evaluation

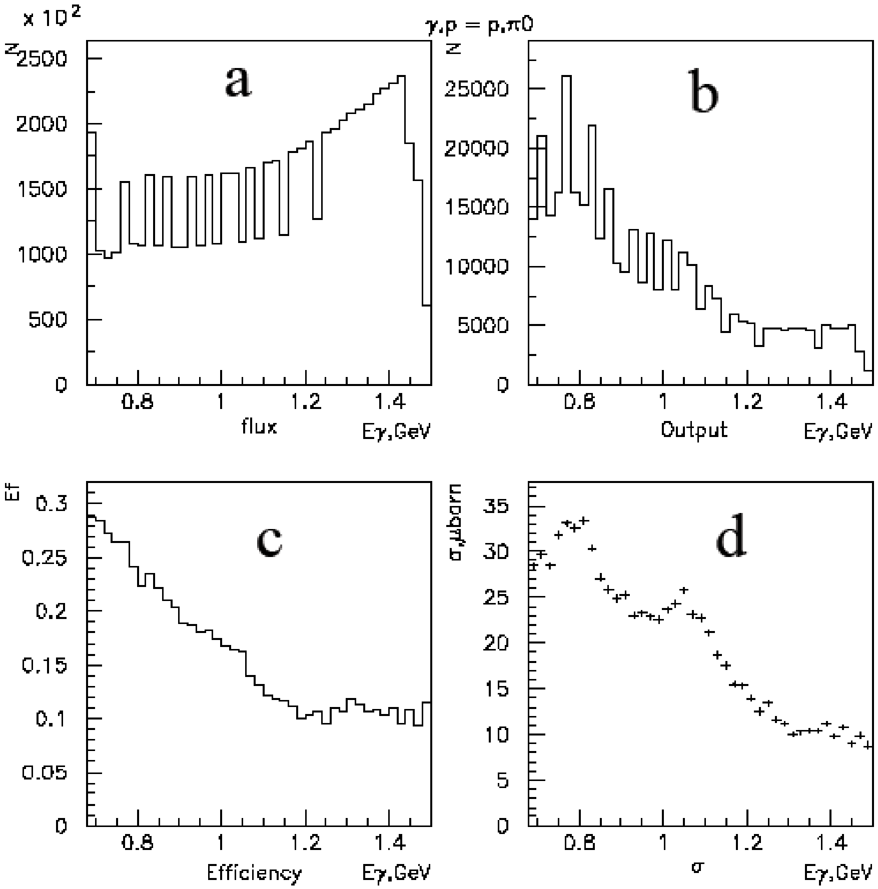

Photon flux (a), yield (b), measurement efficiency (c) (reaction $\gamma p \Rightarrow p\pi^0$). Cross section (d) is obtained by division of the yield on the flux, and normalized on the measurement efficiency and thickness of the target.

Systematic accuracy for $\gamma p > \pi^0 p$

LASER :

GREEN -UV 340 нм

RED - 514 нм

Curve - MAID-2001

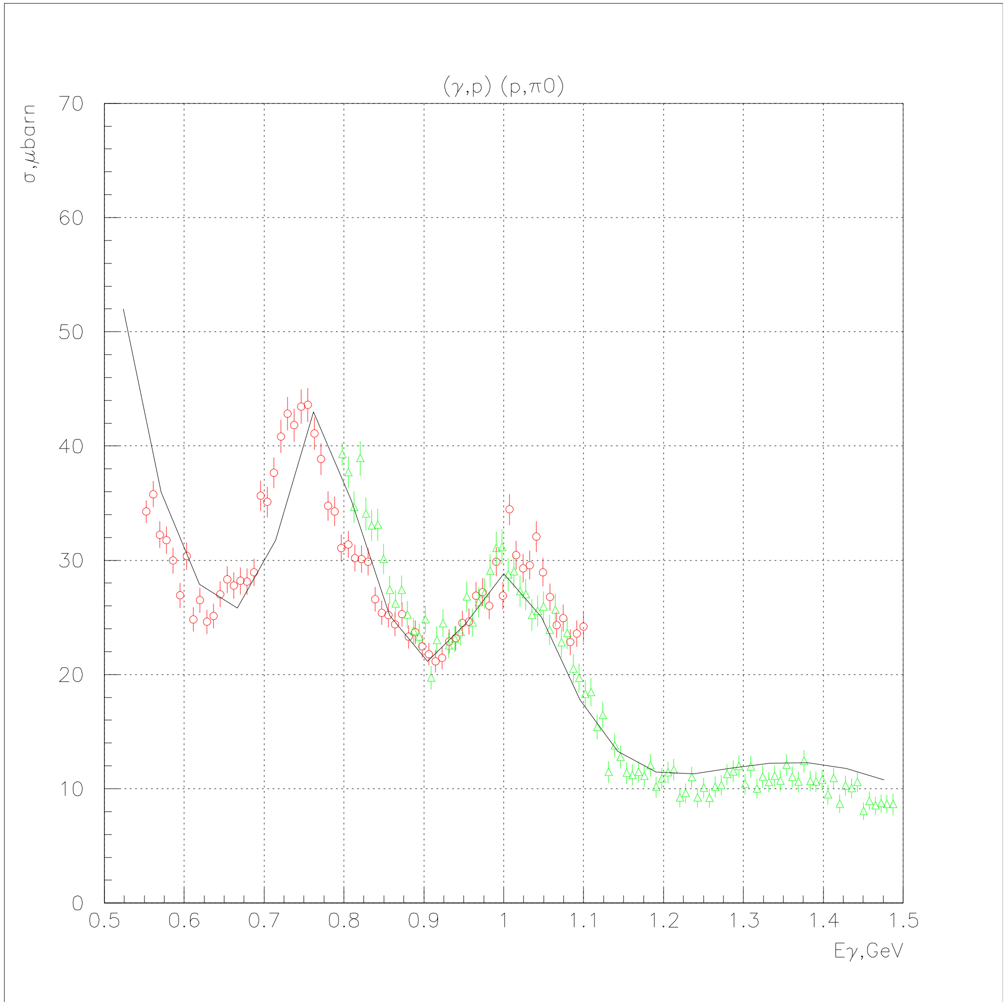

Systematic accuracy for $\gamma p > \pi^+ n$

LASER :

GREEN -UV 340 нм

RED - 514 нм

Curve - MAID-2001

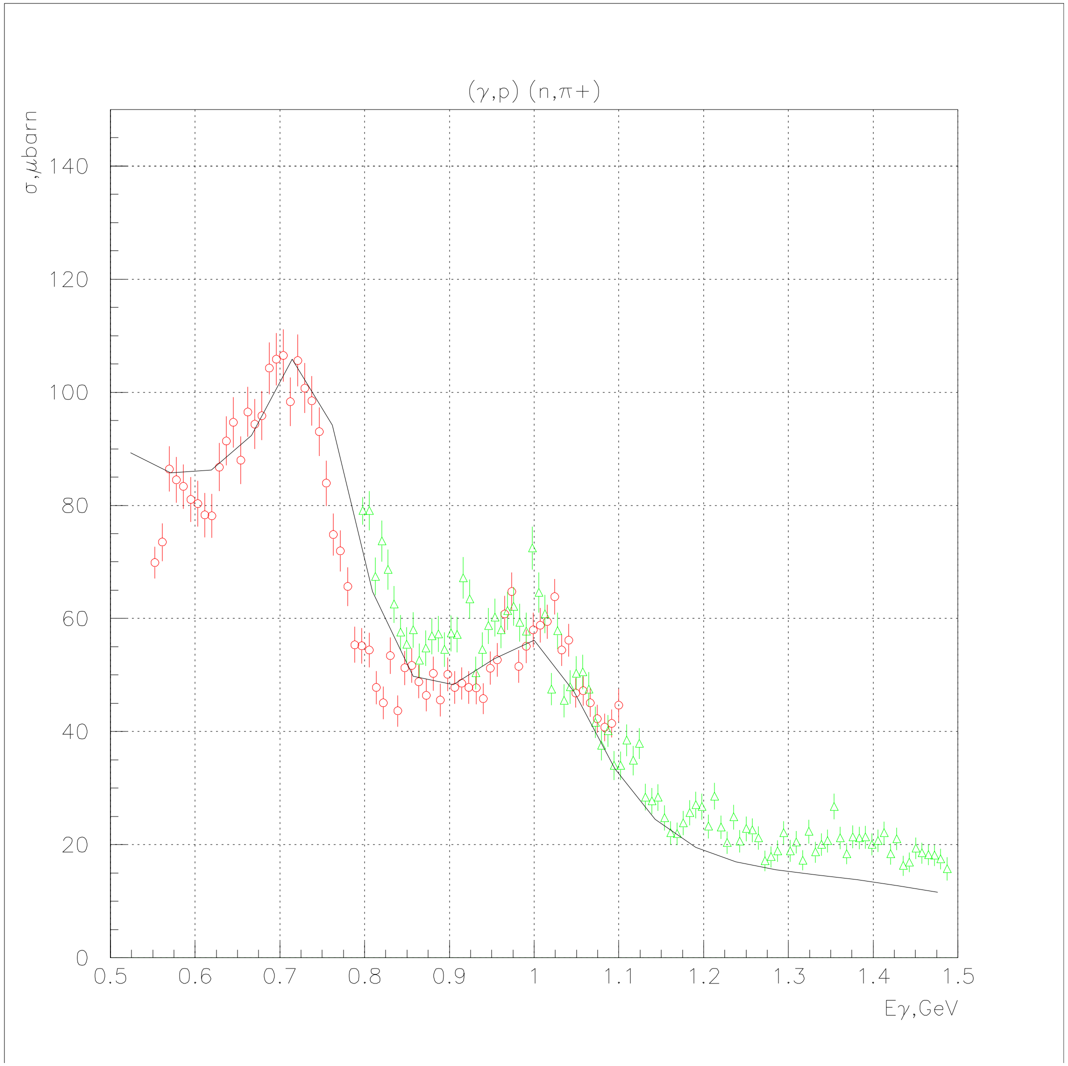

Systematic accuracy for $\gamma p > \pi^+\pi^- p$

LASER :

GREEN -UV 340 нм

RED - 514 нм

Curve - MAID-2001

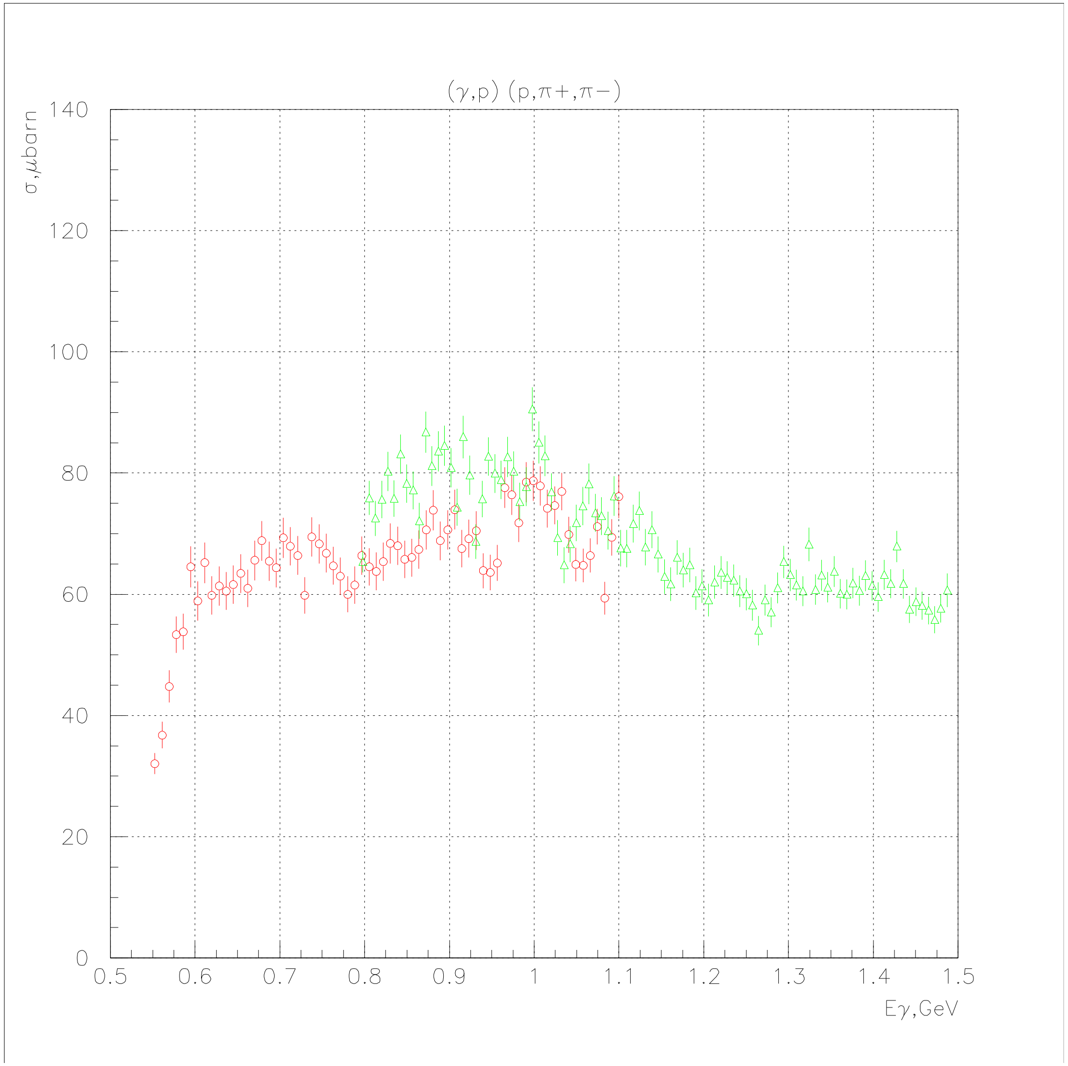

Systematic accuracy for $\gamma p > \pi^0\pi^+ n$

LASER :

GREEN -UV 340 нм

RED - 514 нм

Curve - MAID-2001

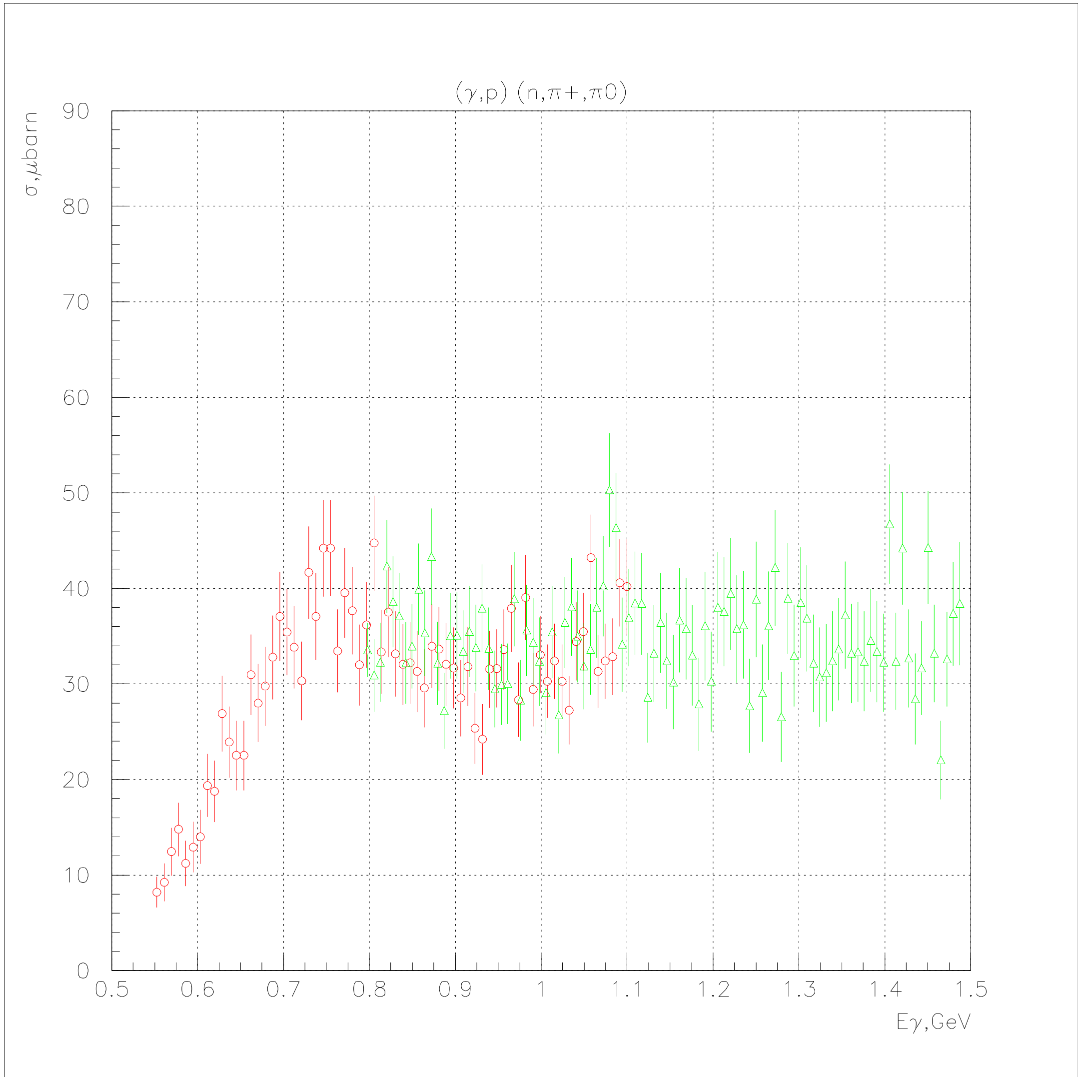

Experimental results

Free proton

Experimental data from

GRAAL (black points – subtraction method) ,

Armstrong (open points) ,

and Mainz (triangles).

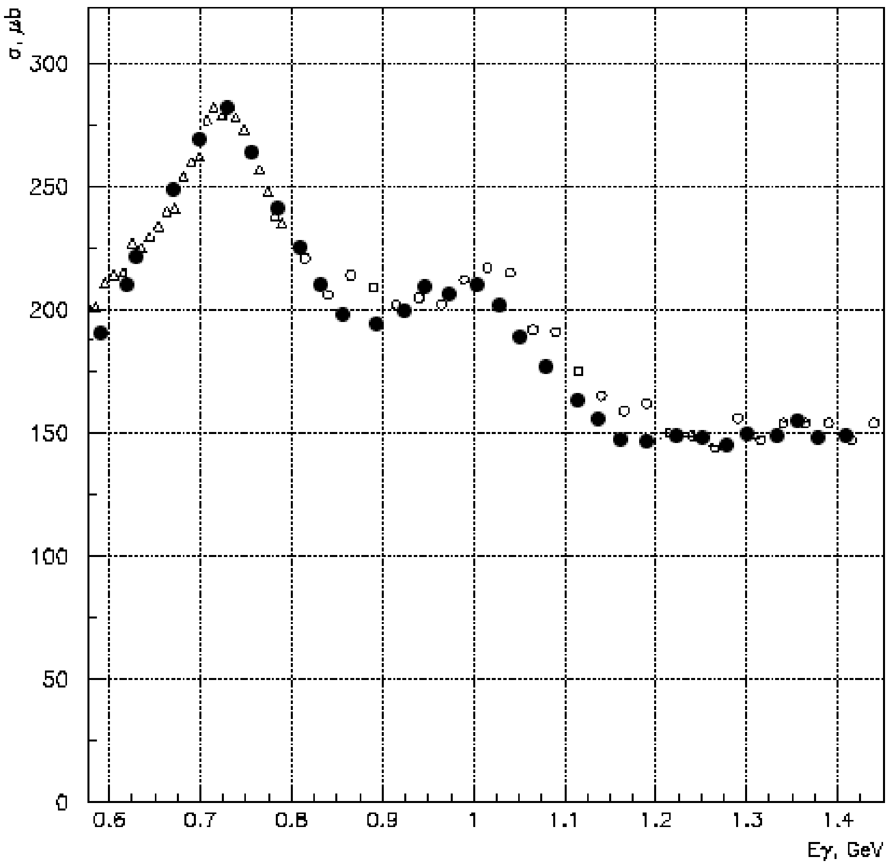

Total photoabsorption cross section for free proton

(subtraction and summing methods) GRAAL-2008

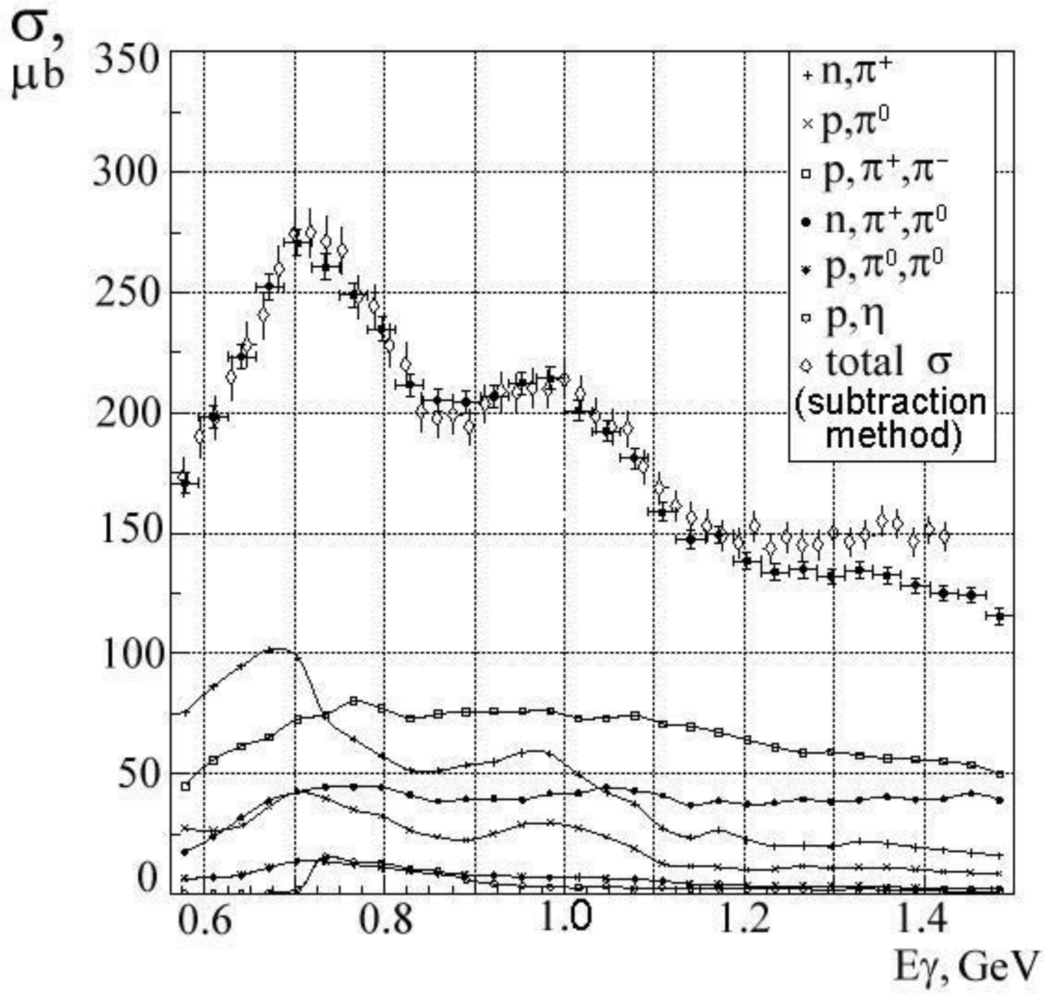

Experimental results
Deuteron

Black points – Armstrong 1972

Open triangles – GRAAL 2009
Subtraction method

Black triangles – GRAAL
Summing method

Expanded scale

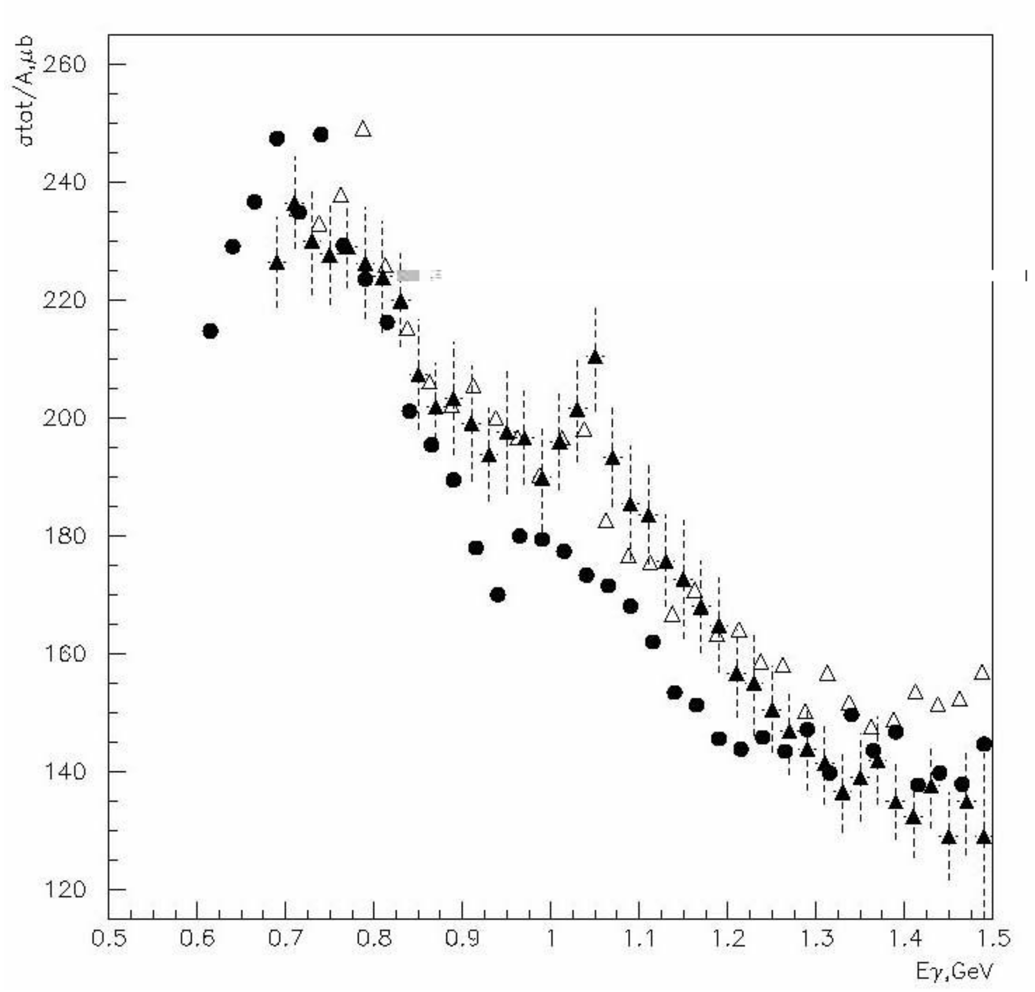

Experimental results

Bound proton

(deuteron target)

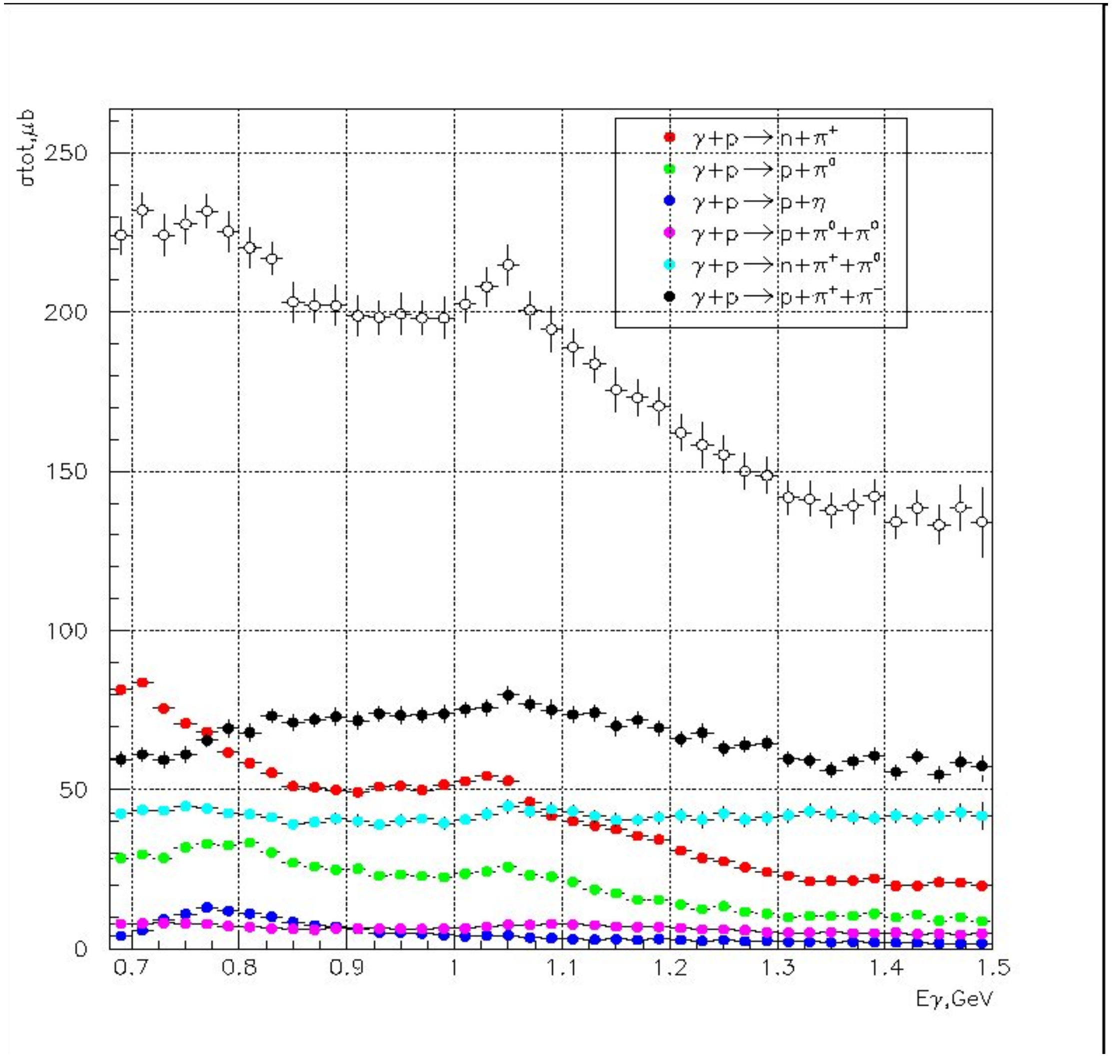

Experimental results

Bound neutron

(deuteron target)

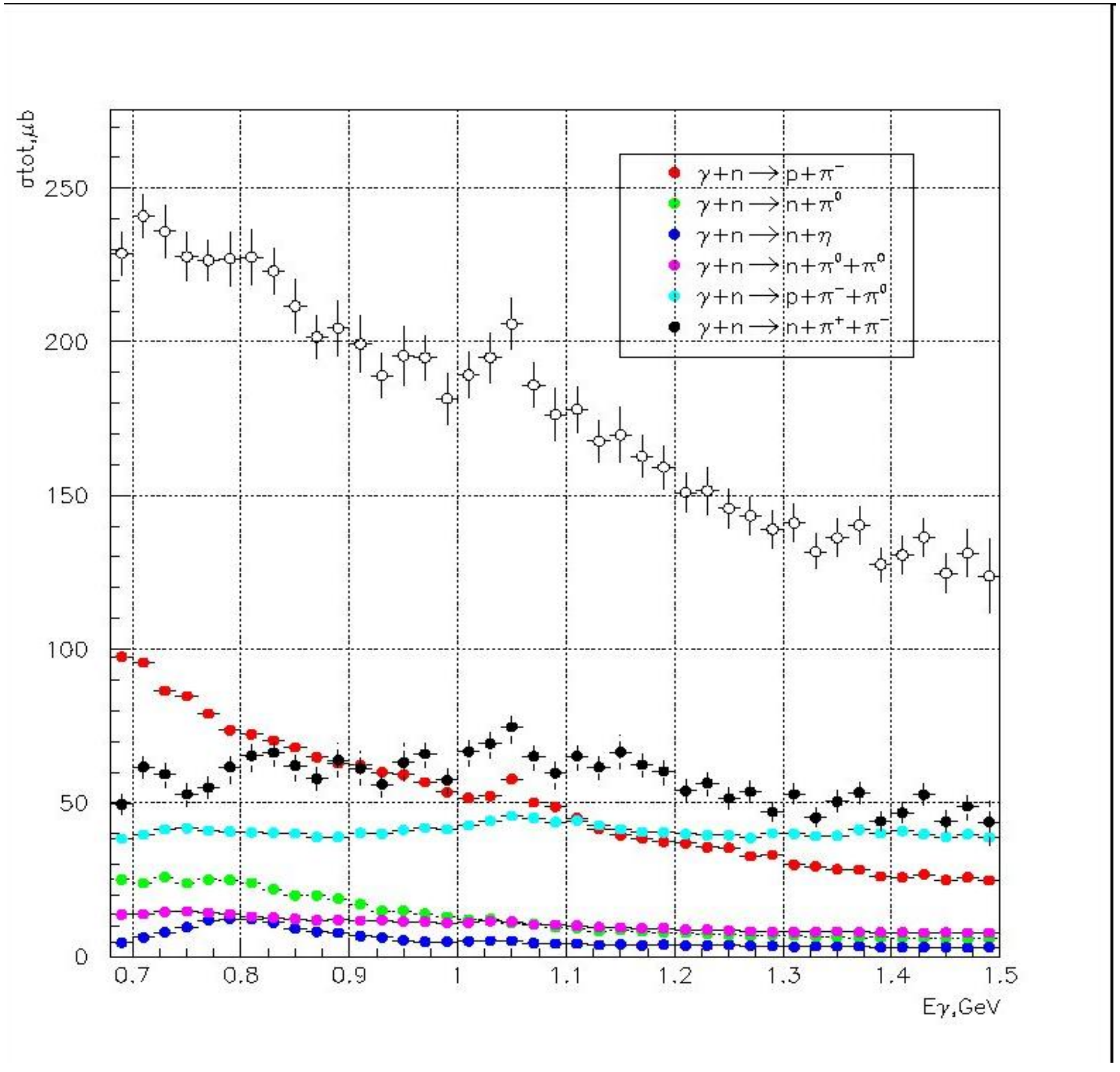

Bound nucleon
(^{2}D and ^{12}C target)

Points – Armstrong (1972) (^{2}D)

Triangles – GRAAL (^{2}D)

Crosses – GRAAL (^{12}C)

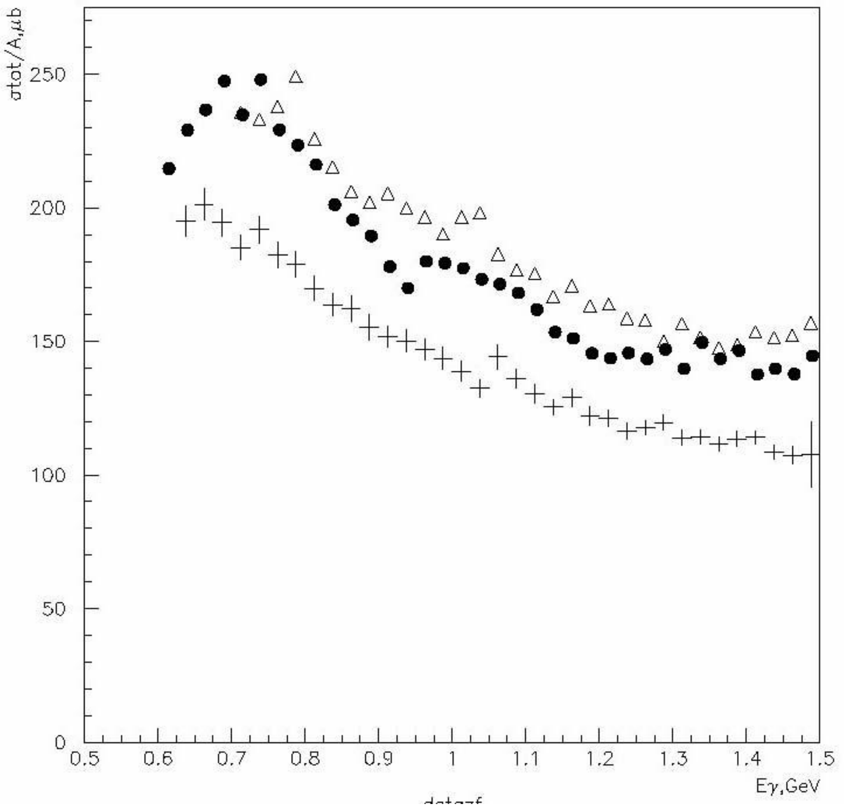

Total photo-absorption cross section for ^{12}C.

Crosses - GRAAL data,

full points – Bianchi e.a. [4]

open points - Mirazita e.a. [5]

“Universal curve” - full line.

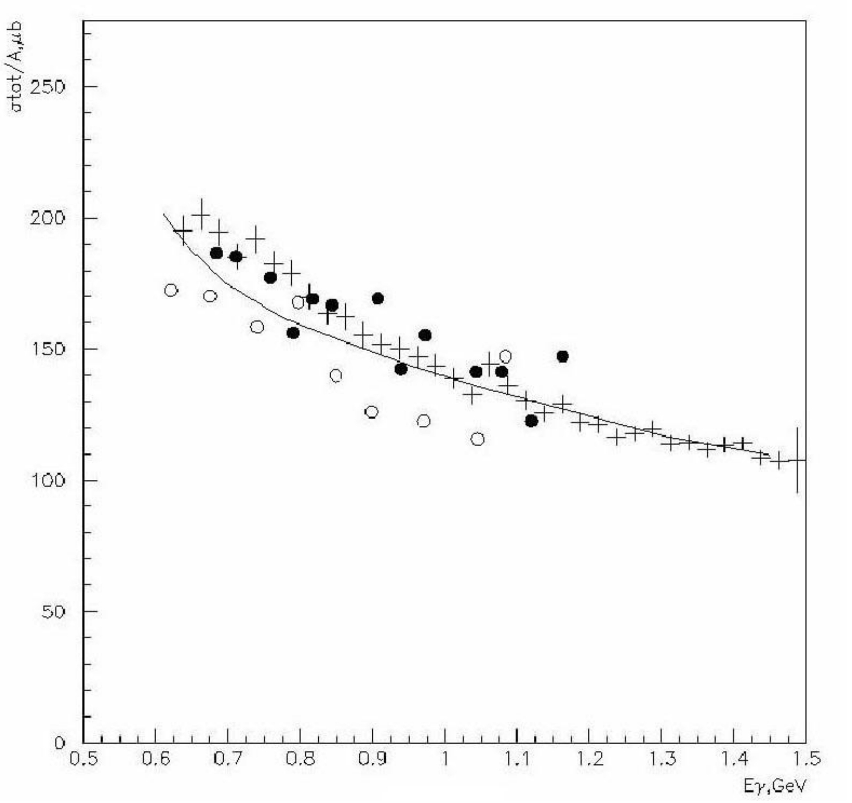

Total photo-absorption cross section for the bound nucleon (deuteron target)

GRAAL data (summing of partial channels)

Green points – proton
Red points - neutron

Equality of p and n cross sections

Indication of the "door-way" states ???

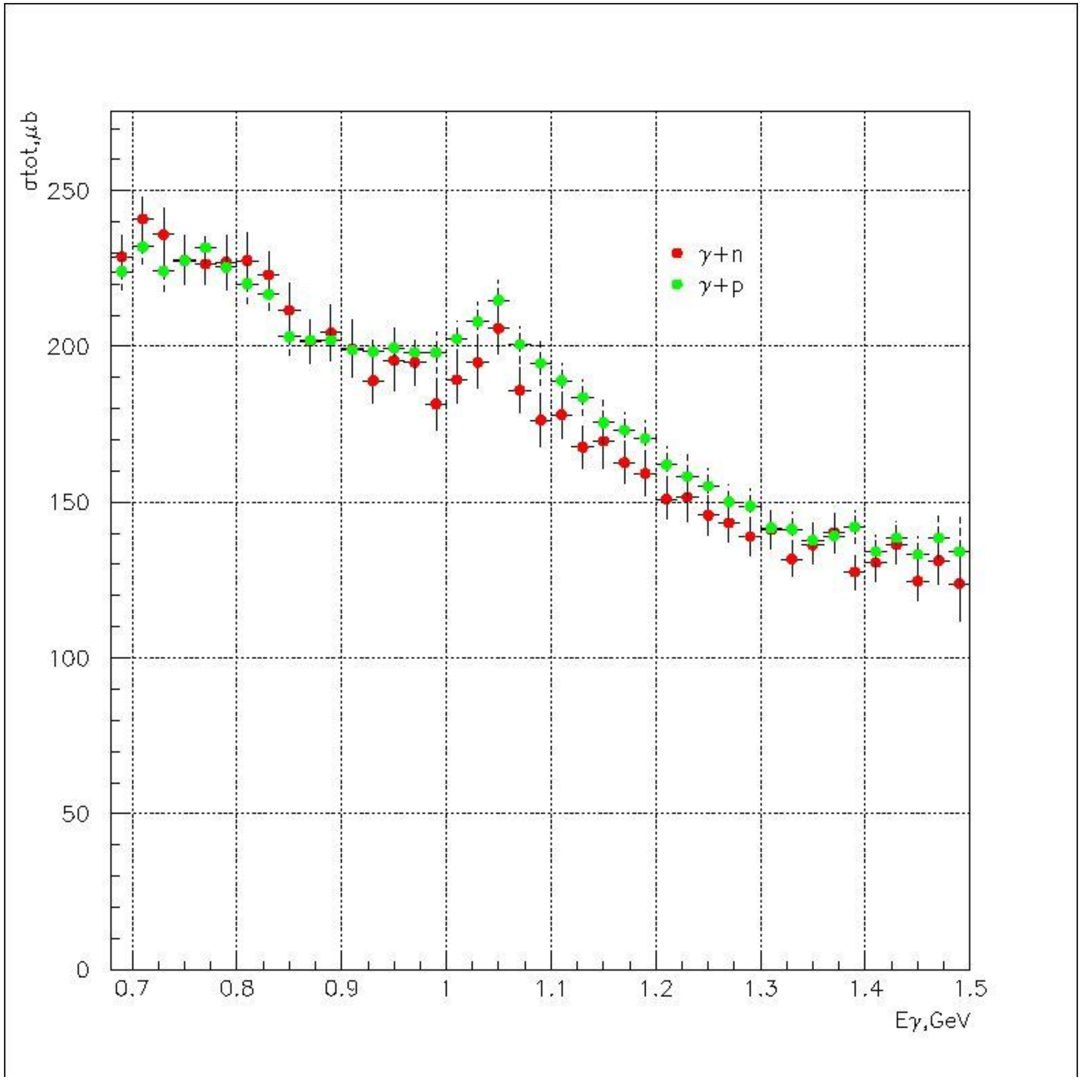

Attempt to get the free neutron cross section (Armstrong-1972)

Subtraction of the proton contribution from the deuteron yield

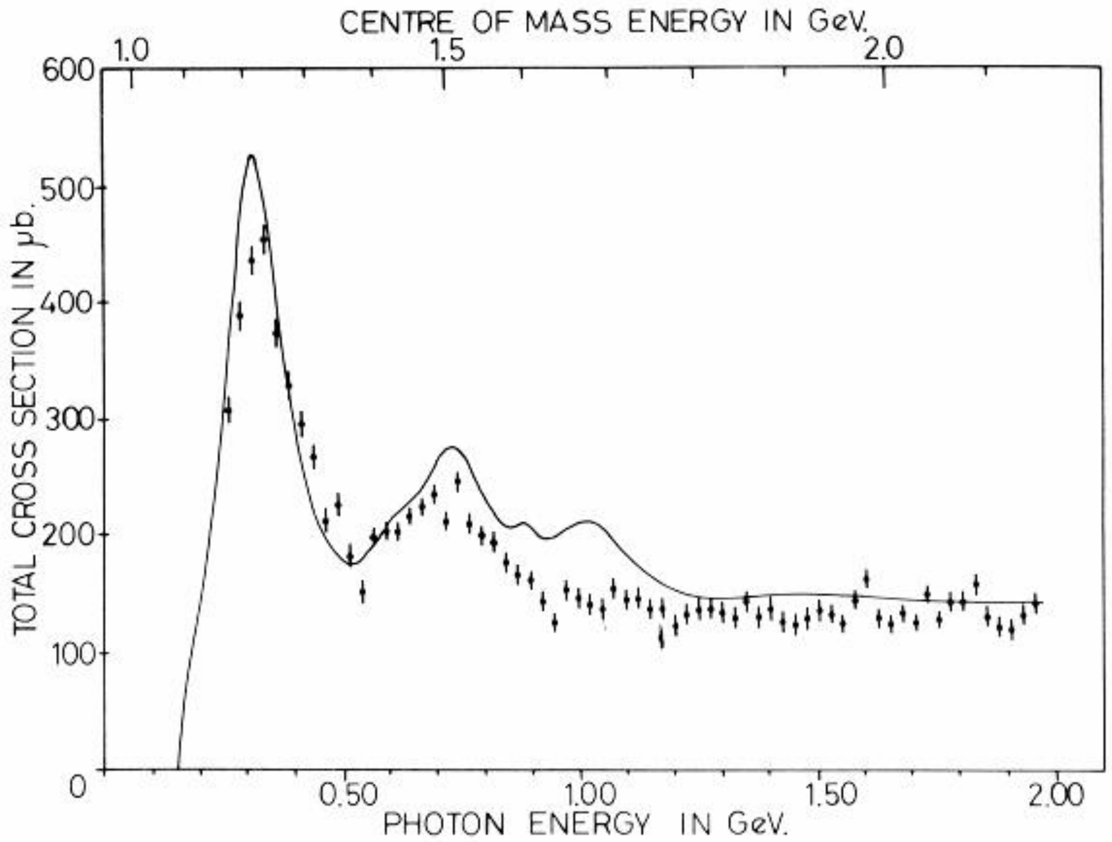

Fig. 8. This shows the values of $\sigma_T{}^n$ in the resonance region obtained by subtracting the measured $\sigma_T{}^p$ values from the deuterium values corrected for internal motion of the nucleons. The solid curve is the smooth fit to the measured $\sigma_T{}^p$ values.

Free and bound proton

(deuteron target)

GRAAL data (summing of partial channels)

Blue points – free proton

Red points – bound proton

Expanded scale

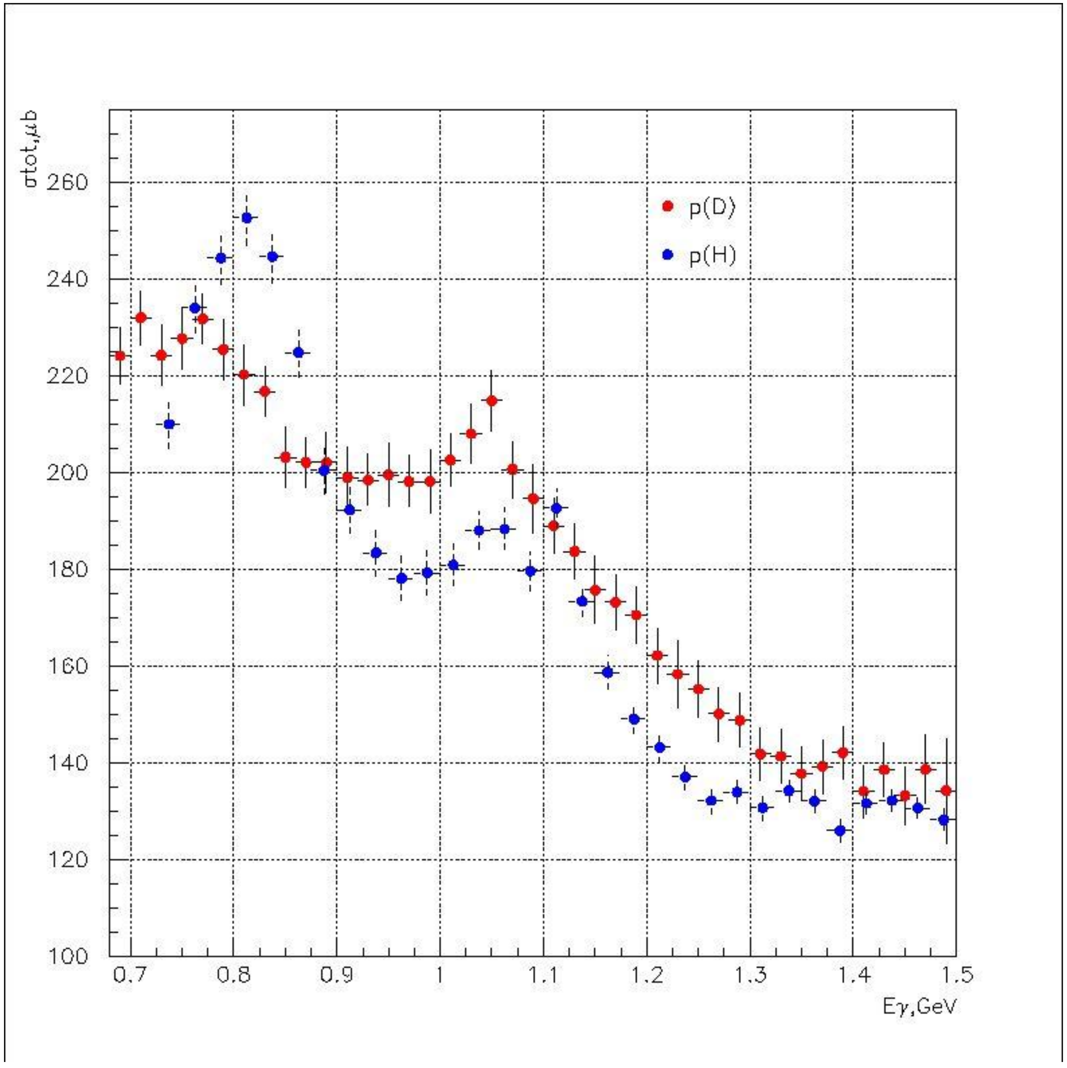

Ratio of free and bound proton photo absorption cross sections

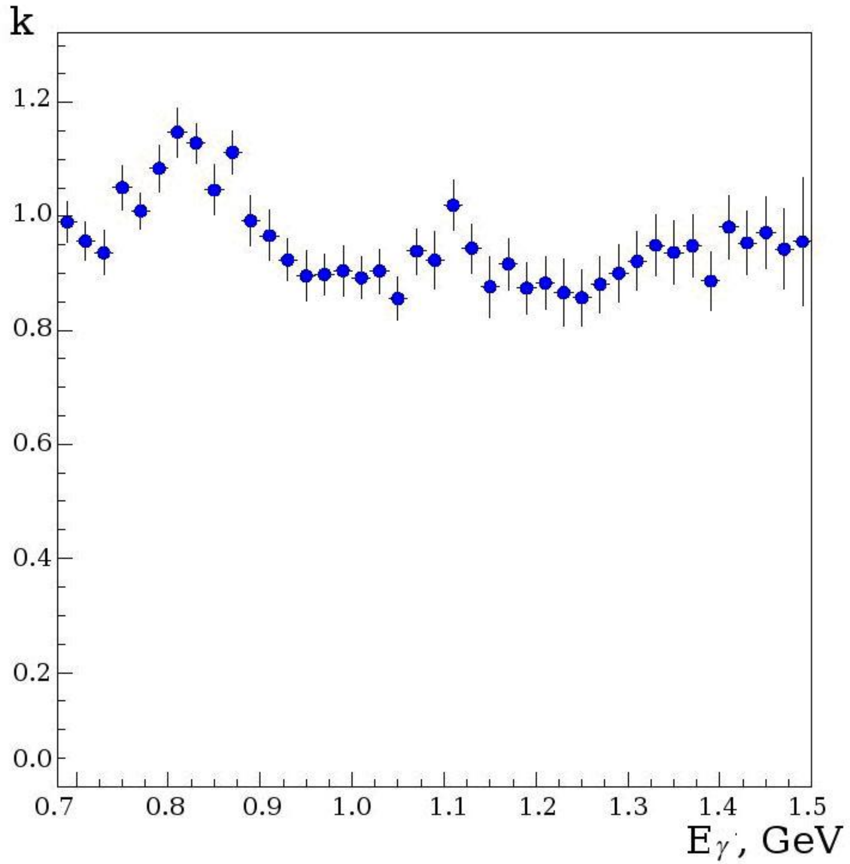

Partial channels for the deuteron
(MAID-2007 for the free nucleon)

$\gamma p > \pi^+ n$

$\gamma n > \pi^- p$

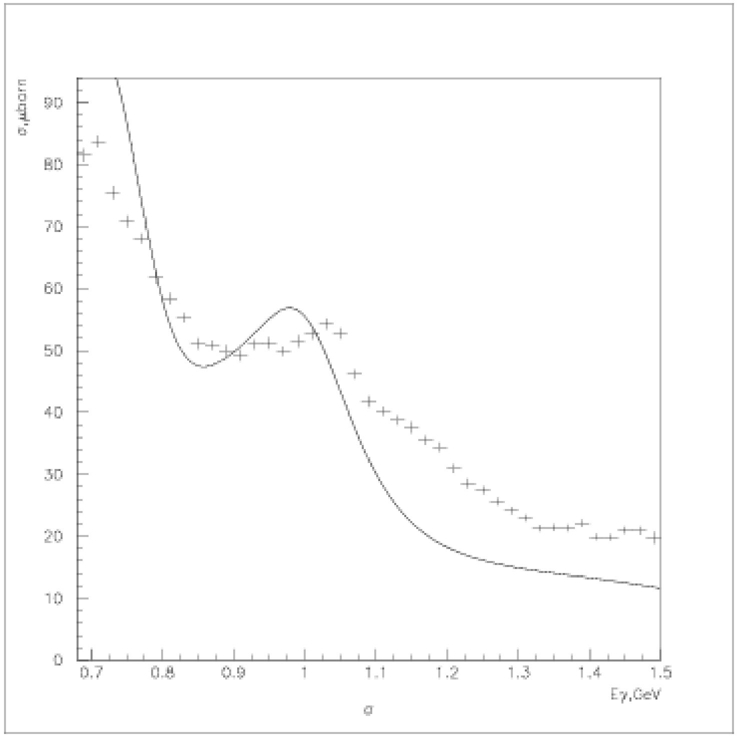

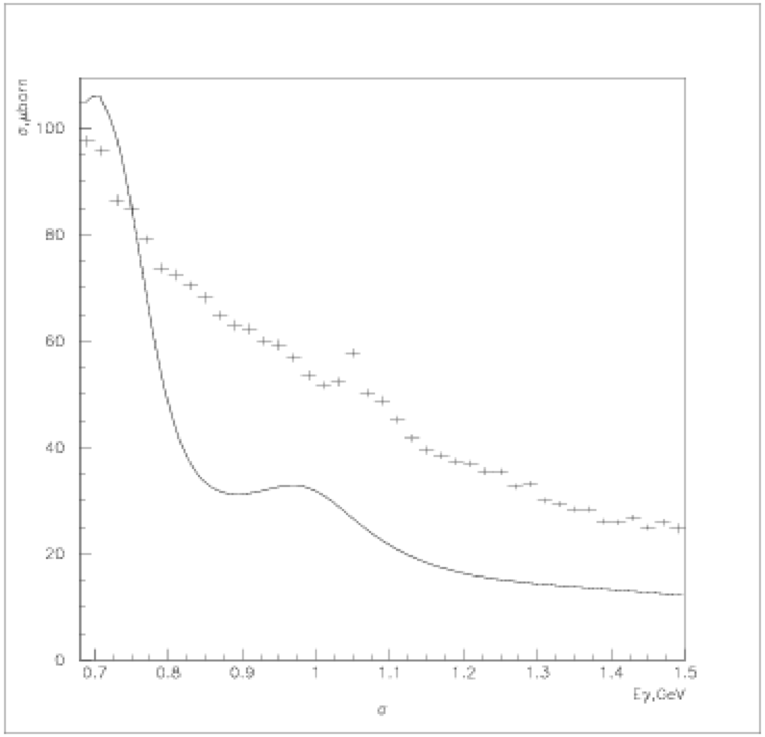

Partial channels for the deuteron
(MAID-2007 for free nucleon)

$\gamma n > \pi^0 n$

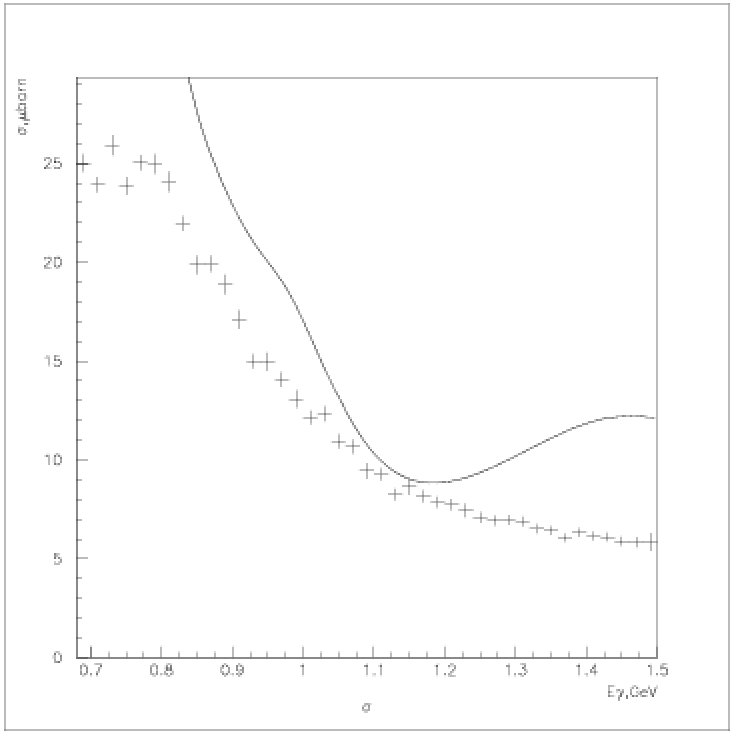

$\gamma p > \pi^0 p$

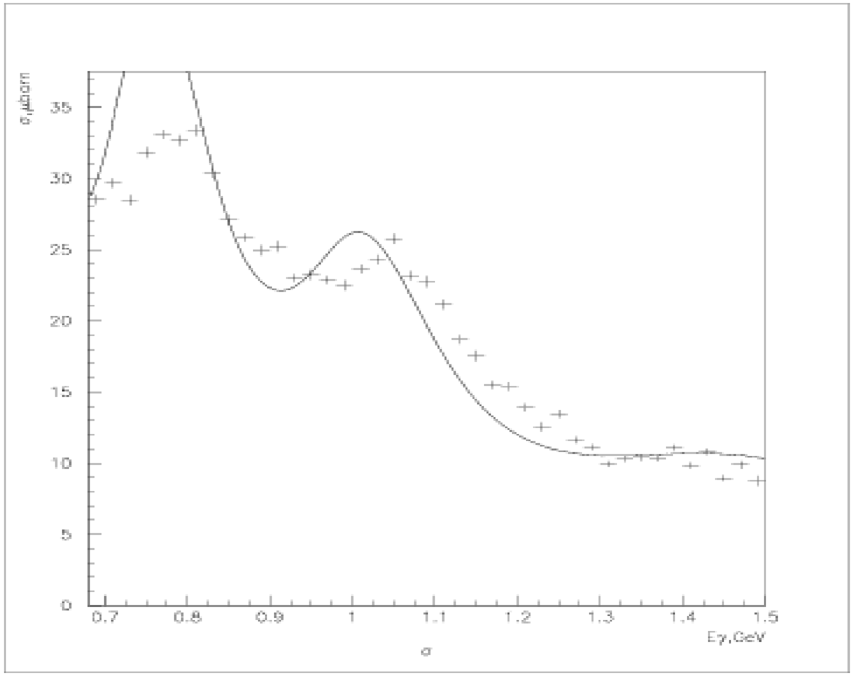

Partial channels for the deuteron
(MAID-2007 for free nucleon)

$\gamma n > \eta\ n$

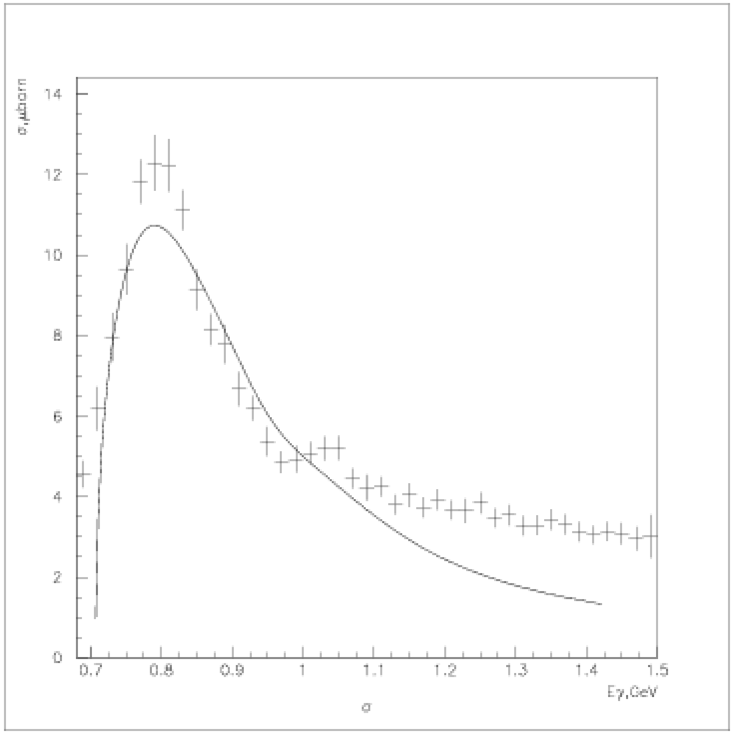

$\gamma p > \eta\ p$

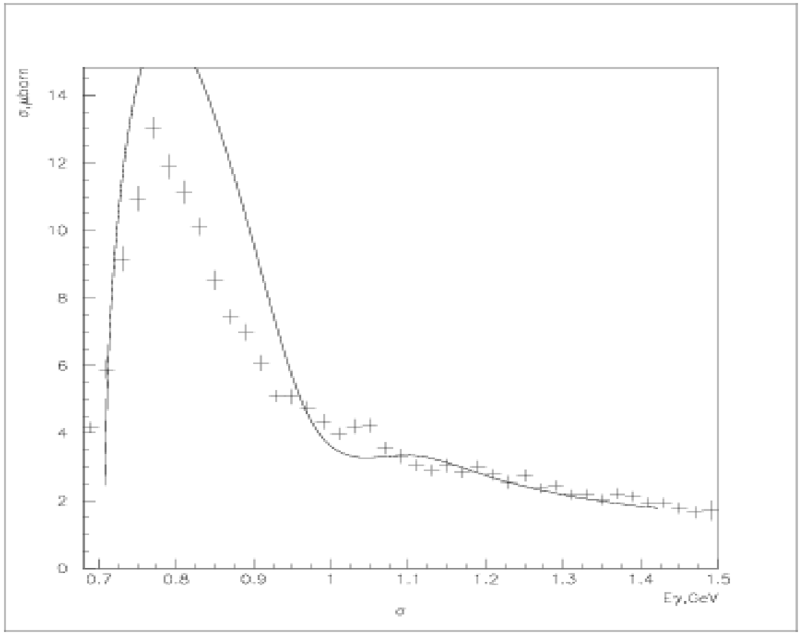

Partial channels for the deuteron
(MAID-2007 for free nucleon)

$\gamma n > \pi^0\pi^0$ n

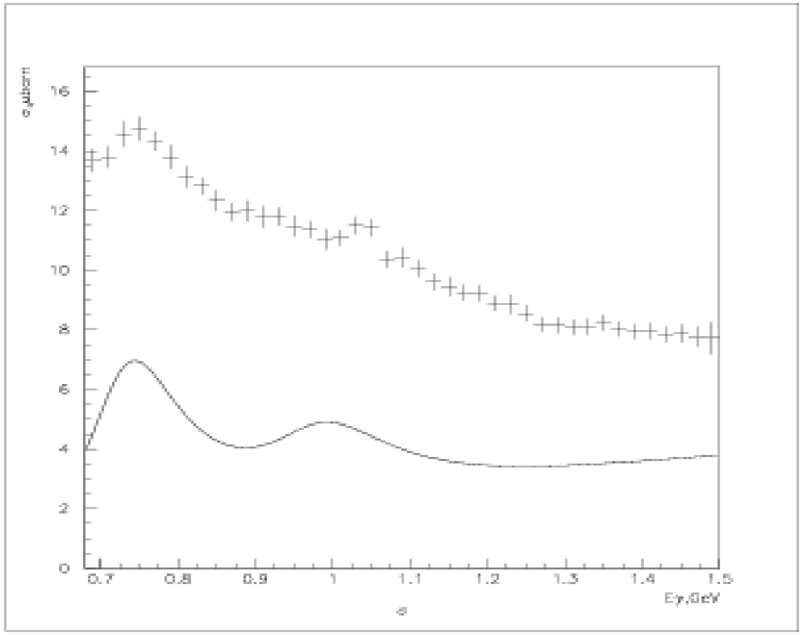

$\gamma p > \pi^0\pi^0$ p

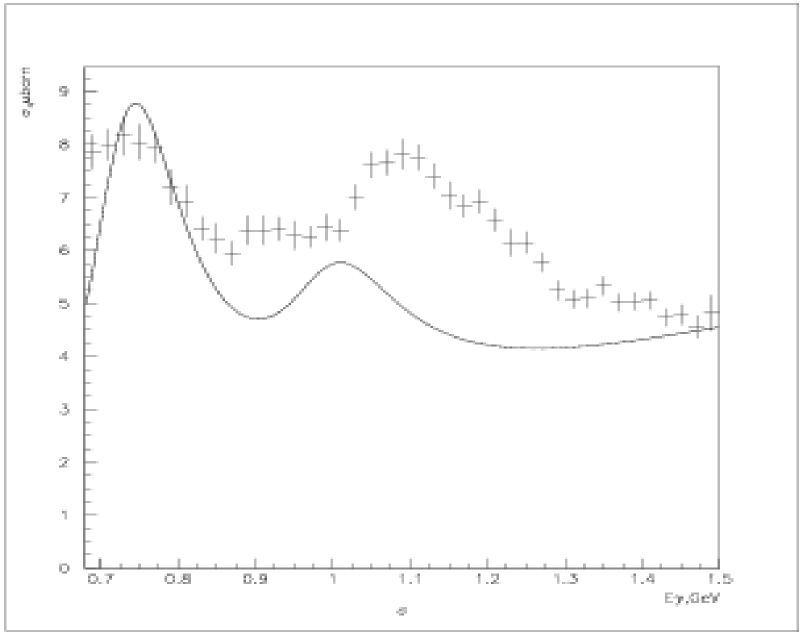

Partial channels for the deuteron
(MAID-2007 for free nucleon)

$\gamma p > \pi^+\pi^0 n$

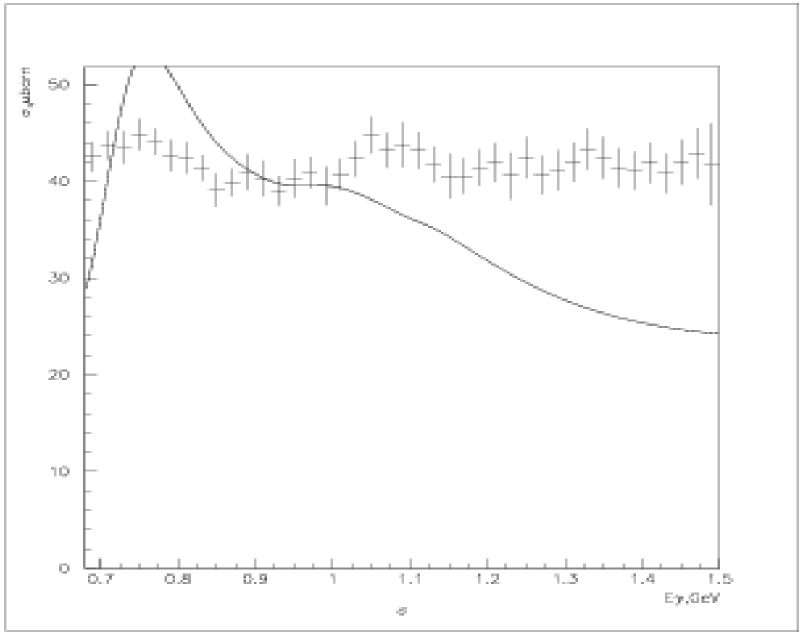

$\gamma n > \pi^-\pi^0 p$

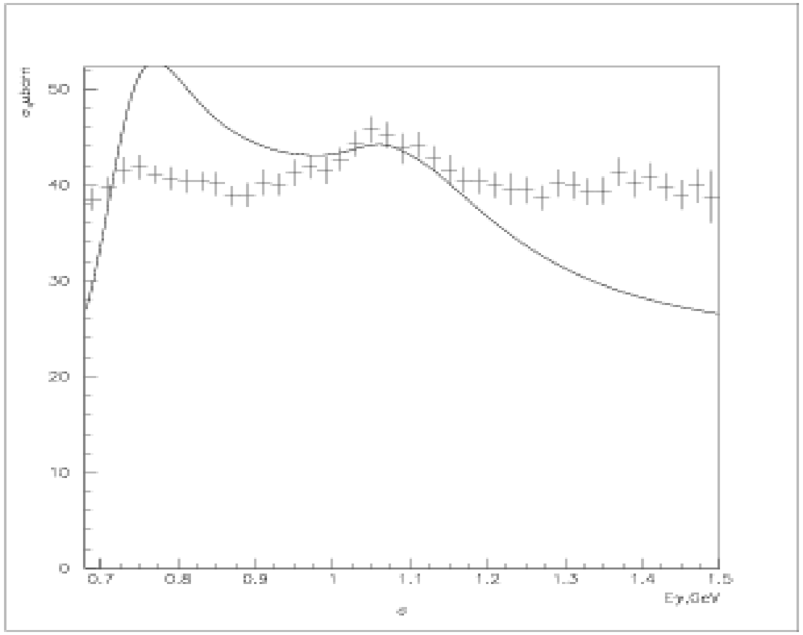

Partial channels for the deuteron
(MAID-2007 for free nucleon)

$\gamma n > \pi^+ \pi^- n$

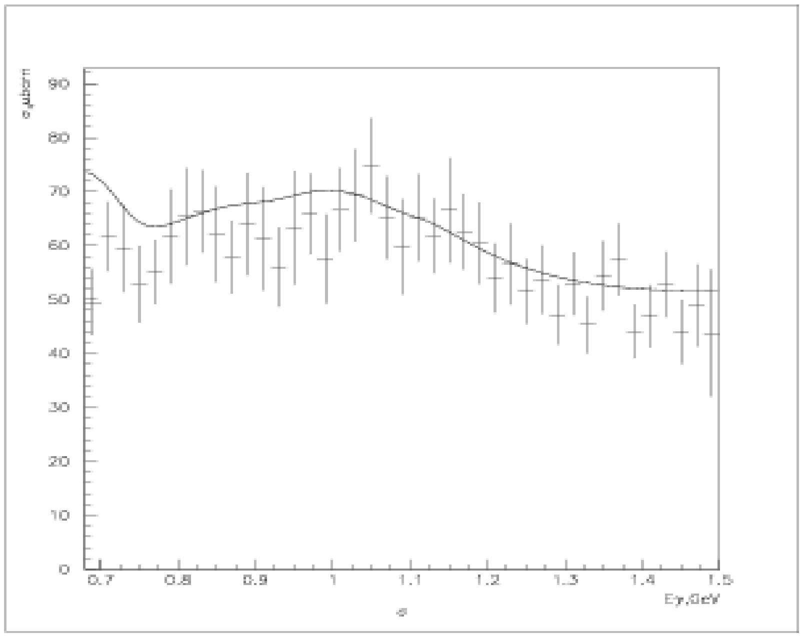

$\gamma p > \pi^- \pi^+ p$

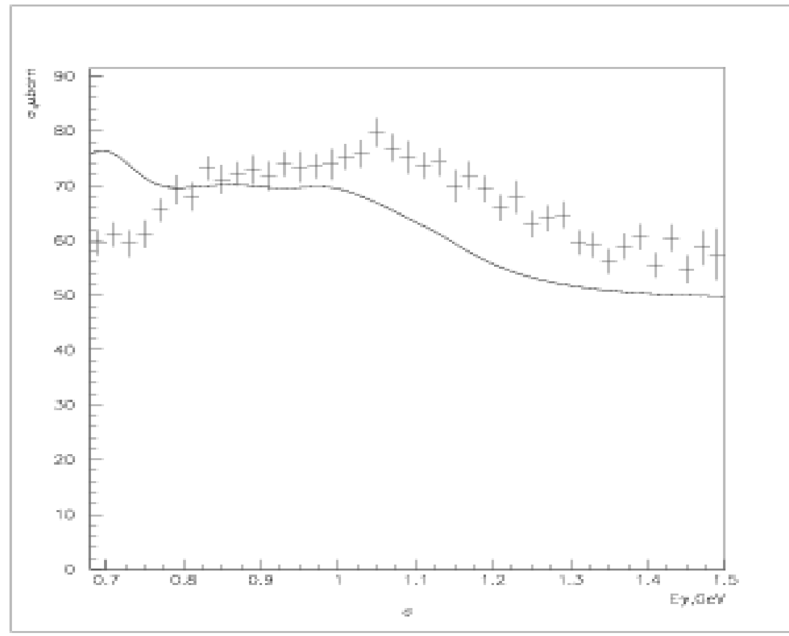

Partial cross sections for one and double pion and η meson photo-production on free and quasi-free proton and quasi-free neutron

Red – free proton, green – quasi-free proton, blue – quasi-free neutron.

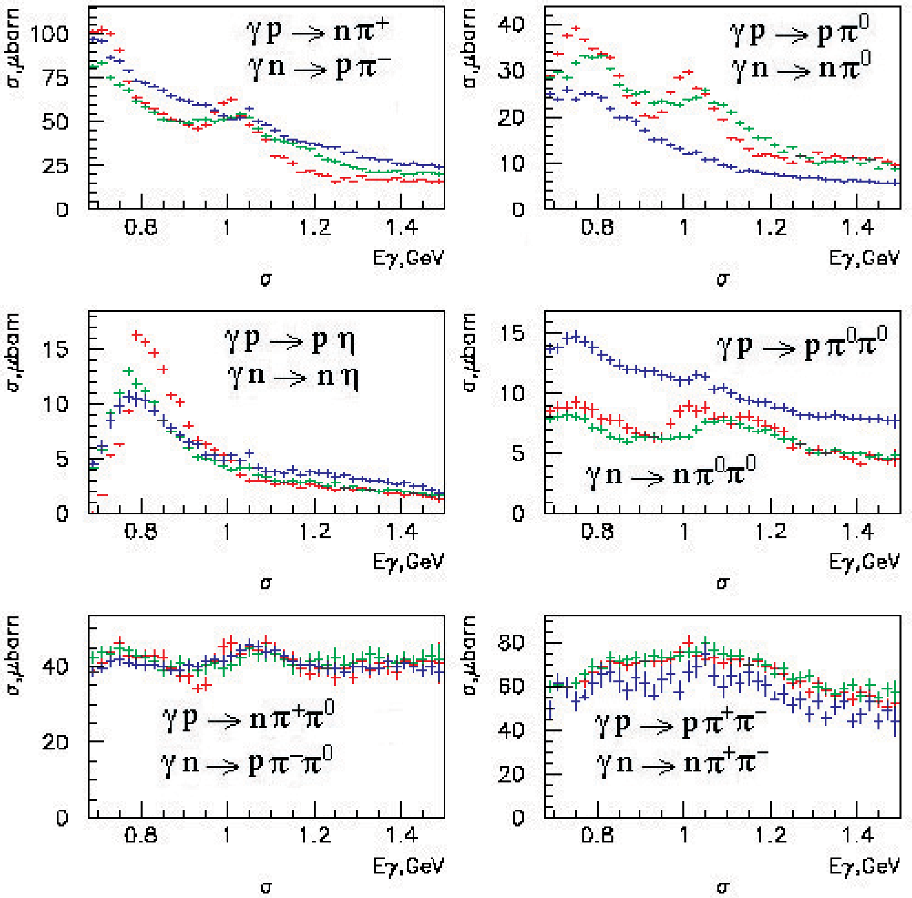

Specific media modification in different channels indicates that two nucleon correlations plays important role in addition to Fermi motion.

Actinide nuclei
(Novosibirsk VEPP-4 -1990, CEBAF - 2000)

Free proton and neutron - dotted line
Actinide nuclei - solid line
Different nuclei with A = 7 – 238
(universal curve) – experimental points

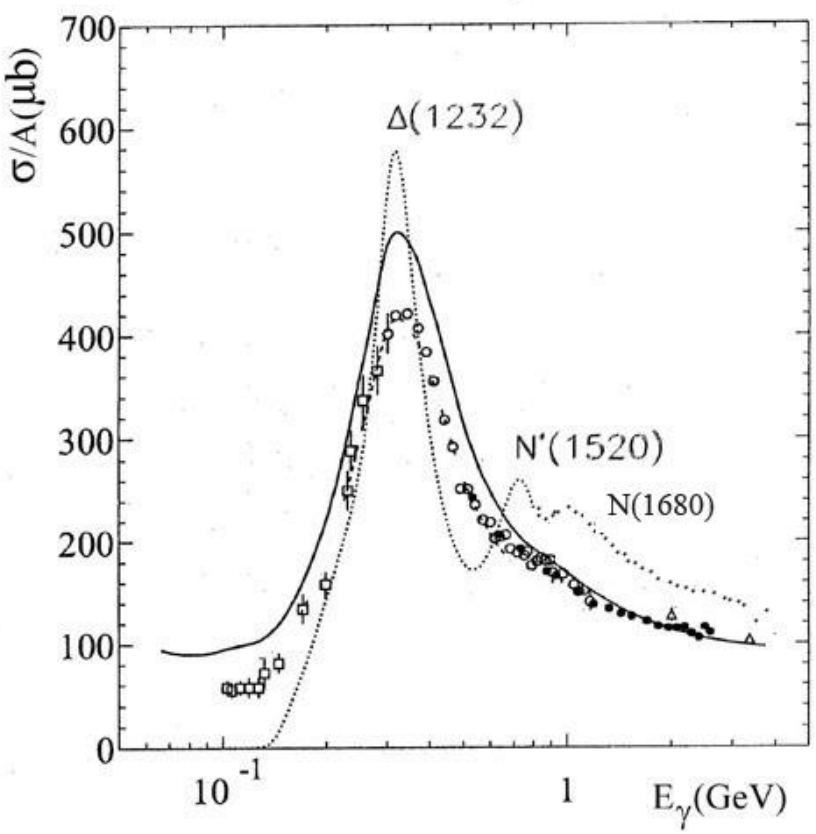

For actinide nuclei:
Excess of 20% in the Δ-resonance region
Width of Δ-resonance is larger.

Unpredictable behavior above Δ- resonance

High order quantum electrodynamics effects

($Z^2\alpha > 1$)

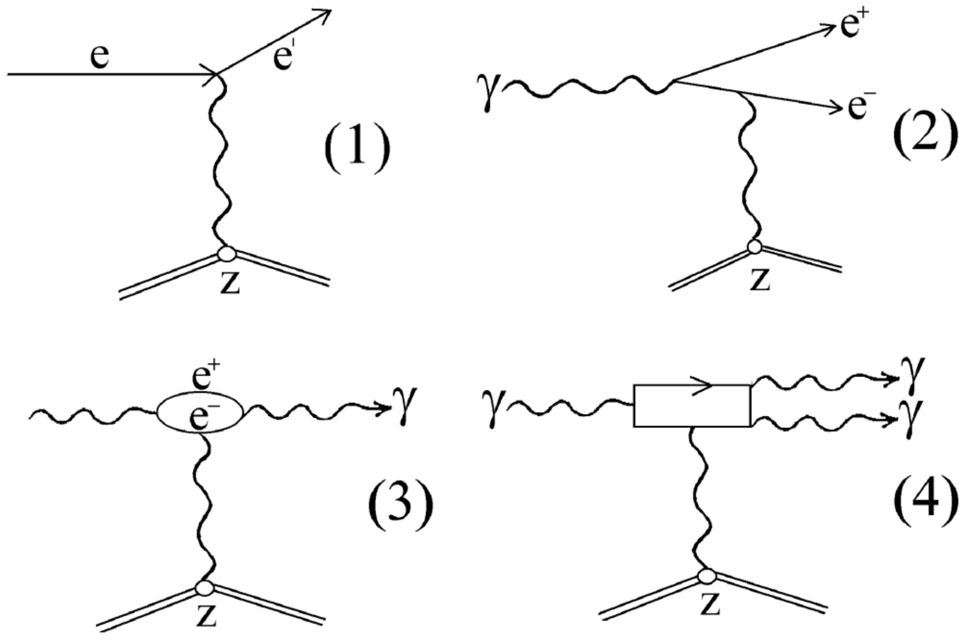

1- Electron scattering, 2 – e+e- pair production ,

3- Delbruck scattering, 4 – photon splitting

Coulomb dissociation

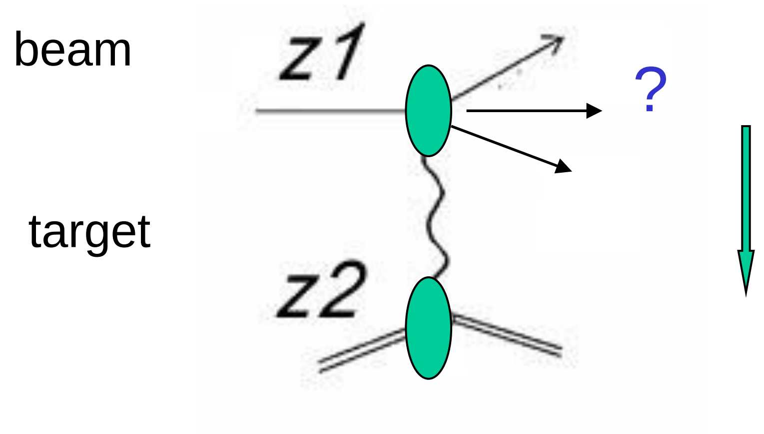

$b > b_{min} = R_i + R_t$ (incident + target)

Virtual photons :

Flux

$$F = \frac{Z^2\alpha}{\pi^2 b^2}\frac{1}{\omega}$$

Energy spectrum (integrated over b), $Z = Z_t$

$$\frac{dn(\omega)}{d\omega} \approx \frac{z^2\alpha}{\pi}\frac{1}{\omega} f\left(\frac{\omega b_{min}}{\gamma}\right)$$

[X.Artru e.a. PL 40B (1972) 43]

New methods are desirable

eA – collider

for stable and exotic nuclei

For NICA

$$E_e \approx 1 GeV, E_{HI} \approx 1 Gev/n$$

Model independent correction on Fermi motion
E_γ and θ^{cm} correction

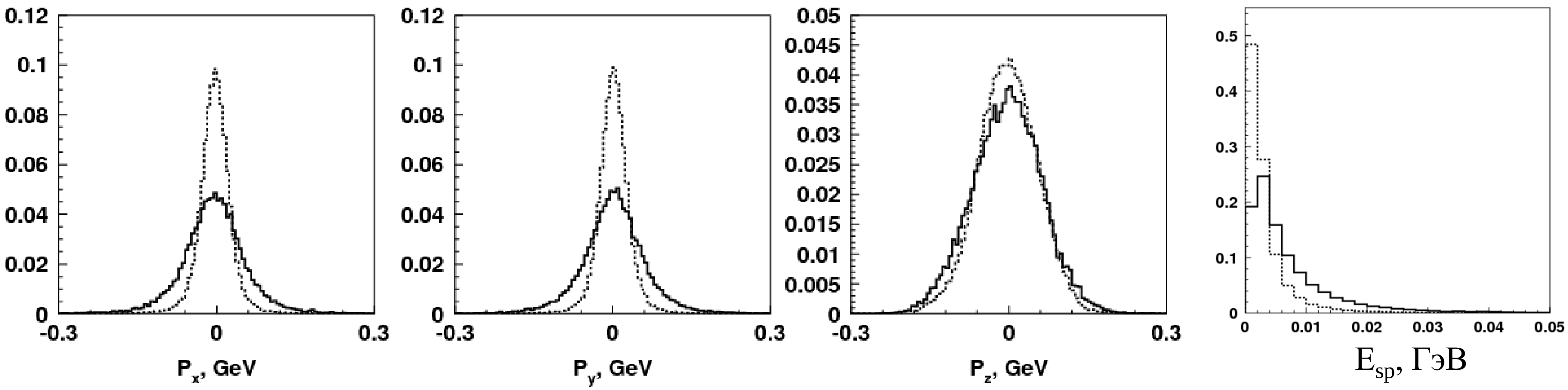

Photoproduction of η-mesons on the deuteron

—— bound proton ------ free proton

Θ^{cm} correction

$$\cos\theta_\eta^{cm} = \frac{(p_\eta^{cm})_z^{corr}}{|(\vec{p}_\eta^{cm})^{corr}|},$$

$$(\vec{p}_\eta^{cm})^{corr} = \gamma_{cm}(\vec{p}_N - \vec{\beta}_{cm}E_N),$$

$$\vec{\beta}_{cm} = \frac{\vec{p}_\gamma + \vec{p}_F}{E_\gamma + E_{sp}},$$

$$\gamma_{cm} = \frac{1}{\sqrt{1-\beta_{cm}^2}}.$$

Effective E_γ evaluation

$$W^2 = (E_\eta + E_N)^2 - (\vec{p}_\eta + \vec{p}_N)^2,$$

$$E_\gamma^* = \frac{W^2 - m_N^2}{2m_N}.$$

Tagging of mesons production by recoil nucleons
$\gamma N > \pi , \eta$

simulation

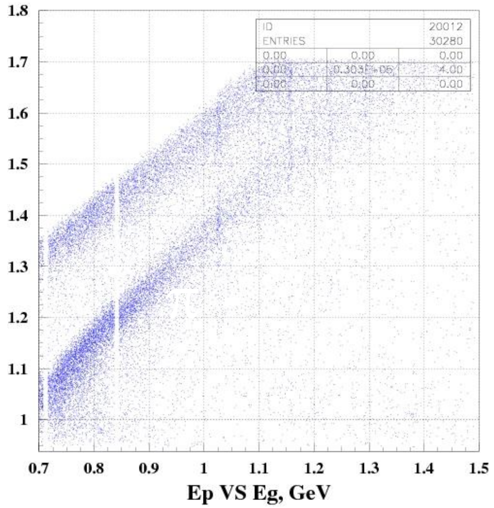

Experiment

Kinematics is not included

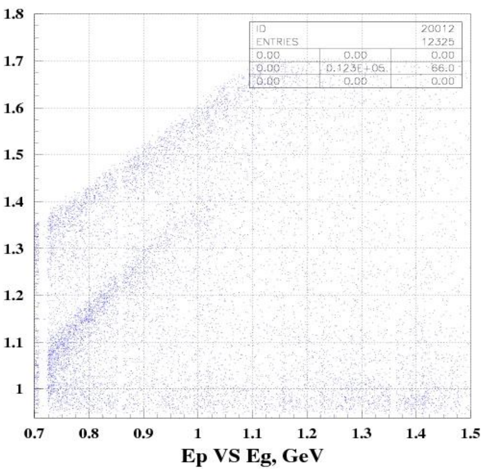

Number of the charged tracks in forward = 1
Number of the neutral clusters in BGO = 2

$2^0 < \text{theta} < 10^0$

GRAAL facility allows to study interaction of unstable mesons with nuclear medium

CONCLUSION

1. Total cross sections for proton and neutron are equal to each other within 5% of experimental accuracy (deuteron target). F15 (1680) resonance is seen in both cross sections.

   This means, probably that

   - free neutron cross section is equal to the free proton one in the nucleon resonance energy region

   - the door-way states in the first step of photon – nucleon interaction which is the sane for the proton and neutron, are possible.

2. Carbon cross section is practically coincides with the “universal curve” but lies in 30% below than the proton and deuteron one.

   This means that only Fermi motion can not explain modification of cross section in nuclear medium, even for light nuclei.

3. Total photoabsorption cross sections of heavy nuclei indicate contribution of high order electrodynamics processes in the Δ–resonance region. . Strong suppression of cross section above 1 GeV is not explained.

4. Exotic narrow resonance are not see neither in total nor in partial cross sections.